Relationships between channelization, sedimentation and sea level in the deltaic environment of the ancient harbor of Lattara, southern France

Jean-Philippe Degeai, Clémence Joseph, Tiphaine Salel, Matthieu Giaime, Nuria Rovira, Gaël Piquès

Relationships between channelization, sedimentation and sea level in the deltaic environment of the ancient harbor of Lattara, southern France

Jean-Philippe Degeai *, Clémence Joseph, Tiphaine Salel, Matthieu Giaime, Nuria Rovira, Gaël Piquès

Archéologie des Sociétés Méditerranéennes UMR5140, Université Montpellier 3, CNRS, Ministère de la Culture, 34000 Montpellier, France

ARTICLE INFO

Editor: Edward Anthony

Keywords:
River delta
Coastal environment
Sedimentology
Harbor engineering
Anthropogenic forcing
Western Mediterranean

ABSTRACT

The impacts of coastal changes and human land use on depositional processes, ecological conditions, geomorphic evolution and harbor works at the archaeological site of Lattara, one of the oldest cities of the northwestern Mediterranean built in a deltaic environment, were investigated from a multi-proxy approach based on sedimentological, biological and geochronological analyses. A distributary channel connected to the ancient harbor of Lattara was deepened and channelized around 200 cal BCE. The drastic increase in water depth caused by channelization was associated with increased flow competence and bedload transport, and could have improved navigation in the harbor area. By contrast, high accumulations of anthropogenic deposits in the channelized stream from the second century CE seem to have negatively affected sediment transport conditions by reducing bedload flux. The construction of a cobble pavement on the western bank of this channelized stream in the fourth century CE was contemporaneous with a sharp decrease in bedload transport showing an abrupt transition to a low energy environment such as in abandoned channels. A drainage ditch was then dug in the deposits of the channelized stream during the Medieval Warm Period, in a context of land use intensification and increased river flooding that led to the deposition of coarser sediments.

1. Introduction

The geographical setting of ancient ports located at the interface between land and sea in the deltaic areas of the Mediterranean was advantageous for commercial activities, but it was also a challenging environment where geomorphic and sedimentary changes related to delta progradation may have caused silting and burying of harbor basins (Marriner and Morhange, 2007; Anthony et al., 2014). Giaime et al. (2019) identified six forcing factors that may have influenced the geomorphological evolution of these ancient harbors: river flooding, sediment inputs, storm events, relative sea-level changes, dredging and harbor works. Moreover, the variation of accommodation space is a geomorphic factor modulating sediment flux in deltaic areas, especially for bayhead deltas in incised-valley systems (Brückner et al., 2005; Clement and Fuller, 2018; Degeai et al., 2020).

Different engineering solutions were developed to face the problem of delta progradation in ancient harbors, such as sediment dredging, canal digging, river channelization, embankment, jetty construction or water diversion. A good example of harbor works and waterway management in a deltaic environment is found in Italy with the port system of ancient Rome, where many geoarchaeological studies revealed the diversity and complexity of engineering strategies used by the Romans to adapt to environmental issues raised by fluvial dynamics or windstorms in the Tiber River delta (e.g. Giraudi et al., 2009; Goiran et al., 2010; Lisé-Pronovost et al., 2019; Vött et al., 2020; Salomon et al., 2023). Another example comes from the Roman harbor of ancient Ephesus (Anatolia), where a canal was built to cope with siltation from the Küçük Menderes (Kaystros) River and to keep the connection between the harbor and the open sea (Stock et al., 2016, 2019).

In southern Gaul the Romans also used a large variety of engineering methods to protect harbors exposed to rapid delta progradation and silting, as in the deltaic plains of the Aude River (Salel et al., 2019) and the Argens River (Bertoncello et al., 2014; Degeai et al., 2020) where high sediment input has strongly affected the ancient ports of Narbonne and Fréjus (Giaime et al., 2019), respectively (Fig. 1A). Embankments and dikes were built along a branch of the Aude River for the former (Sanchez et al., 2016; Faïsse et al., 2018), while dredging and jetty construction were undertaken for the latter (Gébara and Morhange,

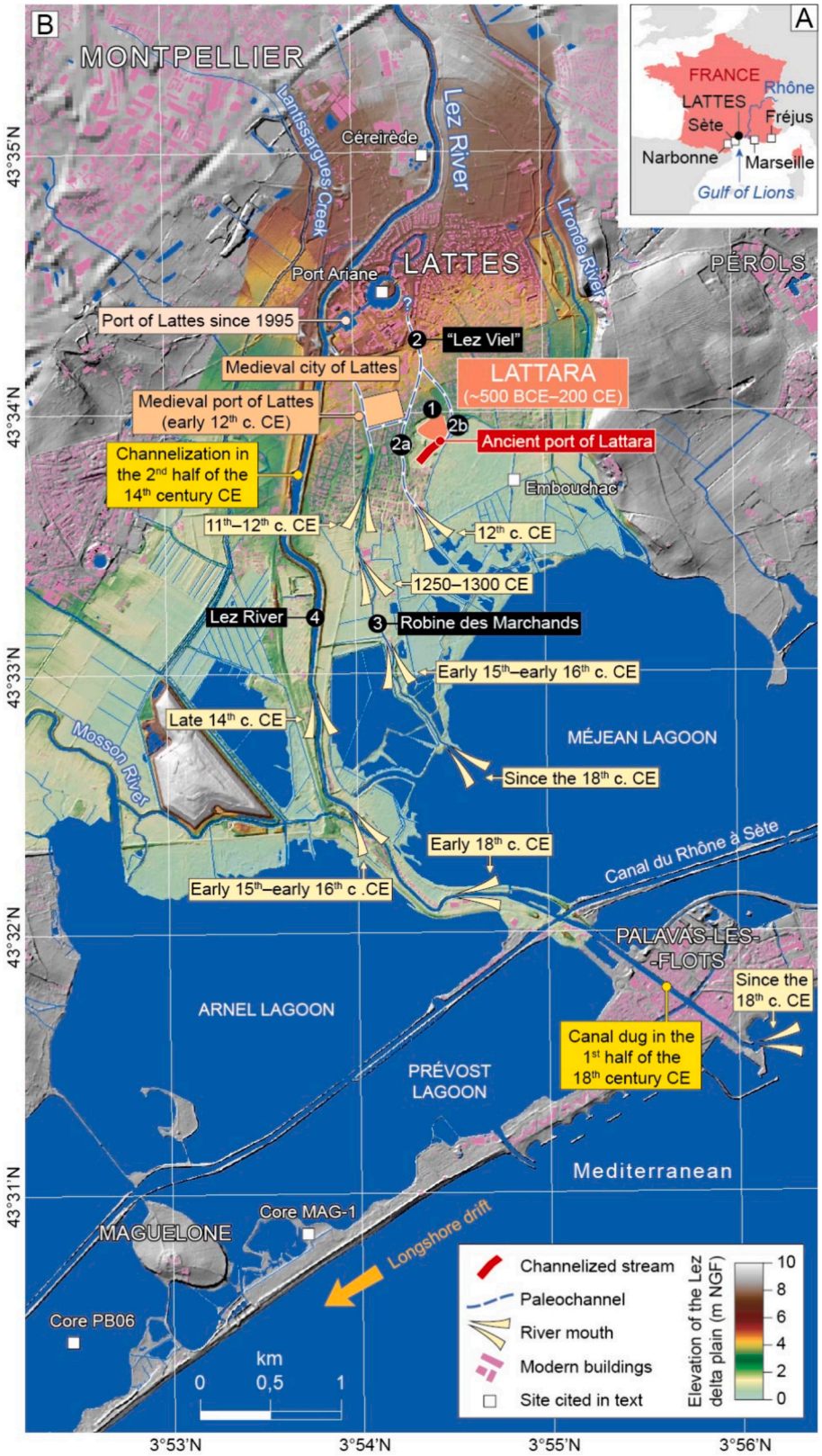

Fig. 1. Location of the ancient city of Lattara and elevation of Holocene sediments in the Lez River delta plain. The ancient fluvial and coastal landforms identified from geoarchaeological studies and the river mouths and channels mentioned in historical maps or texts show a southwestward deltaic progradation over the last three millennia: (1) deltaic lobe on which was built the city of Lattara in the late 6th century BCE (Jorda et al., 2008; Bagan et al., 2010); (2) the "Lez Viel" delta system composed of (a) a western branch active from the 5th century BCE (Jorda et al., 2008) and largely filled in the 12th century CE (Blanchemanche, 2000), and (b) an eastern branch channelized during the Roman period (Py, 1988); (3) the Robine des Marchands channel, along which the medieval port of Lattes was built in the first half of the 12th century CE (Blanchemanche, 2002); (4) the Lez River after channelization west of the medieval port in the 14th century CE then canal digging across the sand barrier at Palavas-les-Flots in the 18th century CE (Blanchemanche, 2000, 2002; Blanchemanche et al., 2004). Westward longshore drift over the last 6000 years from Raynal et al. (2009). Elevation from LiDAR data (Litto3D, SHOM/IGN). NGF: Nivellement Général de la France (French Geodetic Datum).

2010; Bony et al., 2011).

Among the ancient cities of the French Mediterranean coast, Lattara is particularly interesting to study the effects of delta progradation, coastal hazards and land use on waterway management and river engineering over a timespan of almost one millennium. Indeed, the succession of Etruscan, Greek and Roman settlements of this coastal city located in the Lez River delta plain (Fig. 1B) shows that it was inhabited from the late 6th century BCE to the 2nd century CE and then gradually abandoned from the 3rd century CE (Py and Garcia, 1993; Py, 2009).

Port structures in the southern part of the city were dated from the early 2nd century BCE to the end of the 3rd century CE (Garcia and Vallet, 2002; Garcia, 2008). Archaeological excavations undertaken in the 1960s and 1970s revealed the presence of parallel walls interpreted as the remains of a canal or channelized river connected to the port (Arnal et al., 1974; Py, 1988), but it was not extensively studied. Hence a new research project combining archaeological excavations with archaeobotanical and geoarchaeological studies was initiated in 2016 in order to analyze the spatial extent and environmental context of harbor facilities south of Lattara. This research provides an excellent opportunity to study the evolution of one of the oldest harbors identified in the northwestern Mediterranean, both before and after the Roman conquest of southern Gaul that occurred in the late 2nd century BCE (Christol, 2010).

Here we use a multidisciplinary approach based on new sedimentological, biological, geochronological and archaeological data to study how coastal changes and land use may have impacted sedimentary dynamics, waterway management and harbor works at Lattara. More specifically, the main objectives of this paper are to: 1) understand the geomorphic setting of the stream connected to the ancient harbor of Lattara at the time of its channelization until abandonment and re-use in medieval times, 2) estimate the variation of water depth in the channelized stream and its relation to sea level changes and sediment accretion, and 3) identify the role of environmental factors on the evolution of sediment dynamics south of Lattara.

2. Environmental and archaeological contexts

The archaeological site of Lattara is located in the city of Lattes and lies in the coastal plain of the Lez River, which flows into the Gulf of Lions in southern France (Fig. 1). This 28 km long river drains an area of 173 km^2 before its confluence with the Mosson River. The mean discharge rate of the Lez River exhibits a value of 2.5 $m^3 \bullet s^{-1}$ at Montpellier from instrumental data over the last 70 years (source: DREAL Languedoc-Roussillon, https://www.hydro.eaufrance.fr, stream gauging station Y3204030). The French Mediterranean river basins can be affected by extreme rainfall events that cause floods in the coastal plains, especially in autumn (Blanchemanche, 2009; Degeai et al., 2022). The 100-year flood discharge at Montpellier is estimated at 900 $m^3 \cdot s^{-1}$ (DDTM, 2013), i.e. 360 times higher than the mean annual discharge.

The small basin of the Lez River is composed of Mesozoic and Cenozoic sedimentary rocks and sediments. The Holocene alluvial and marsh deposits that constitute the present-day coastal plain in the lower valley south of Montpellier do not exceed 10 m in elevation. These are surrounded by Pliocene continental sediments to the west and by Pleistocene alluvial terraces to the east. Lagoonal sediments deposited in the lower valley of the Lez River during the transgression related to the post-glacial sea level rise show that a back-barrier lagoon reached the site of Lattara in the past (Ambert and Arthuis, 1995; Jorda et al., 2008; Bagan et al., 2010). The formation of the coastal barrier that led to lagoon closure began around 7500 cal BP about 1 km off the present coastline, then the sand barrier retrograded from ca. 5500 cal BP and reached the coring site MAG-1 east of Maguelone (Fig. 1B) around 1800 cal BP (Raynal et al., 2009, 2010). Deltaic progradation over the last millennia created a bayhead delta composed of several distributary channels and river mouths.

The ancient port of Lattara was classified as either a lagoonal harbor (Morhange et al., 2015) or a river mouth harbor (Giaime et al., 2019). In both cases high sediment supply is an important forcing factor controlling the geomorphic evolution in the harbor area (Morhange et al., 2015; Giaime et al., 2019). This is why the ancient port of Lattara is currently landlocked in the Lez delta plain and >1 km away from the edge of Méjean Lagoon. Paleogeographic reconstructions suggested that the development of terrestrial ecosystems occurred from the 3rd century BCE in the southern part of Lattara (Jorda et al., 2008). This is consistent with archaeological data that did not reveal the presence of human settlement before the 3rd century BCE in this area (Fig. 2).

The port underwent several reorganizations until the 3rd century CE (Garcia and Vallet, 2002; Garcia, 2008). The quays in the southern part of the port and the wall found in excavation GAP9/9bis formed an ENE-WSW depression partially filled with coarse alluvial deposits mainly in the 1st century BCE (Arnal et al., 1974), while sediments in excavations 37/2 and 37/3 suggest the presence of a lagoonal environment with fluvial influence in the southeastern area of Lattara at the same time (Jorda, 2002). The ancient port would therefore have been located near a river mouth along a lagoon.

Two parallel walls spaced 15 m apart were identified in excavation GAP22 and supposed to be a part of a canal southwest of the ancient port of Lattara (Py, 1988). New archaeological excavations and geophysical surveys revealed the presence of a paleochannel connected to this ancient port (Piquès, 2016, 2019). More specifically, excavations at Zone 205 show two series of parallel walls or linear structures surrounding the deposits of a stream channelized in several steps from the late 3rd to the late 1st centuries BCE.

3. Materials and methods

3.1. Sediment sampling

The geoarchaeological study of a transverse section through the channelized stream south of Lattara was undertaken from sediment cores and archaeological excavations (Figs. 2–3). Four cores were collected in the central part of the stream (LAP03) and on its eastern (LAP01–02) and western (LAP04) banks using a percussion corer (Atlas Copco Cobra TT) equipped with 1 or 2 m-long window samplers. A Russian corer was used to collect core S1 under section 205S13 between walls MR205012 and MR205002. Sediment samples were also taken in sectors 1d and 5a under anthropogenic deposits dating from the 2nd and 1st centuries BCE (road VO205096).

3.2. Radiocarbon dating

The radiocarbon age of 45 samples of terrestrial material (charcoal, seed, wood, plant debris) was measured by Accelerator Mass Spectrometry at DirectAMS Laboratory (Bothell, USA) and Radiocarbon Poznan Laboratory (Table 1). Radiocarbon ages were calibrated using the IntCal20 calibration curve (Reimer et al., 2020) with Calib v8.2 (calib.org, Stuiver and Reimer, 1993). Five age models and sediment accumulation rates were calculated using linear interpolation and median ages in Table 1, except for samples at −1.36, −2.01 and − 2.45 m NGF in core LAP02 that show age discrepancies probably caused by large uncertainties on the Hallstatt plateau (Van der Plicht, 2004) and for which mean ages of 600, 700 and 745 cal BCE were calculated from the youngest (648–547 cal BCE), entire (823–573 cal BCE) and oldest (772–717 cal BCE) ranges of the 95.4% probability interval, respectively. Besides, we have excluded three radiocarbon dates showing inconsistent ages probably due to either reworking of older organic material (seed in unit US205046 of section 205S04) or sediment contamination by younger organic material provided by deep-rooted plants (plant debris at −3.02 and − 3.47 m NGF in cores LAP02 and LAP03, respectively).

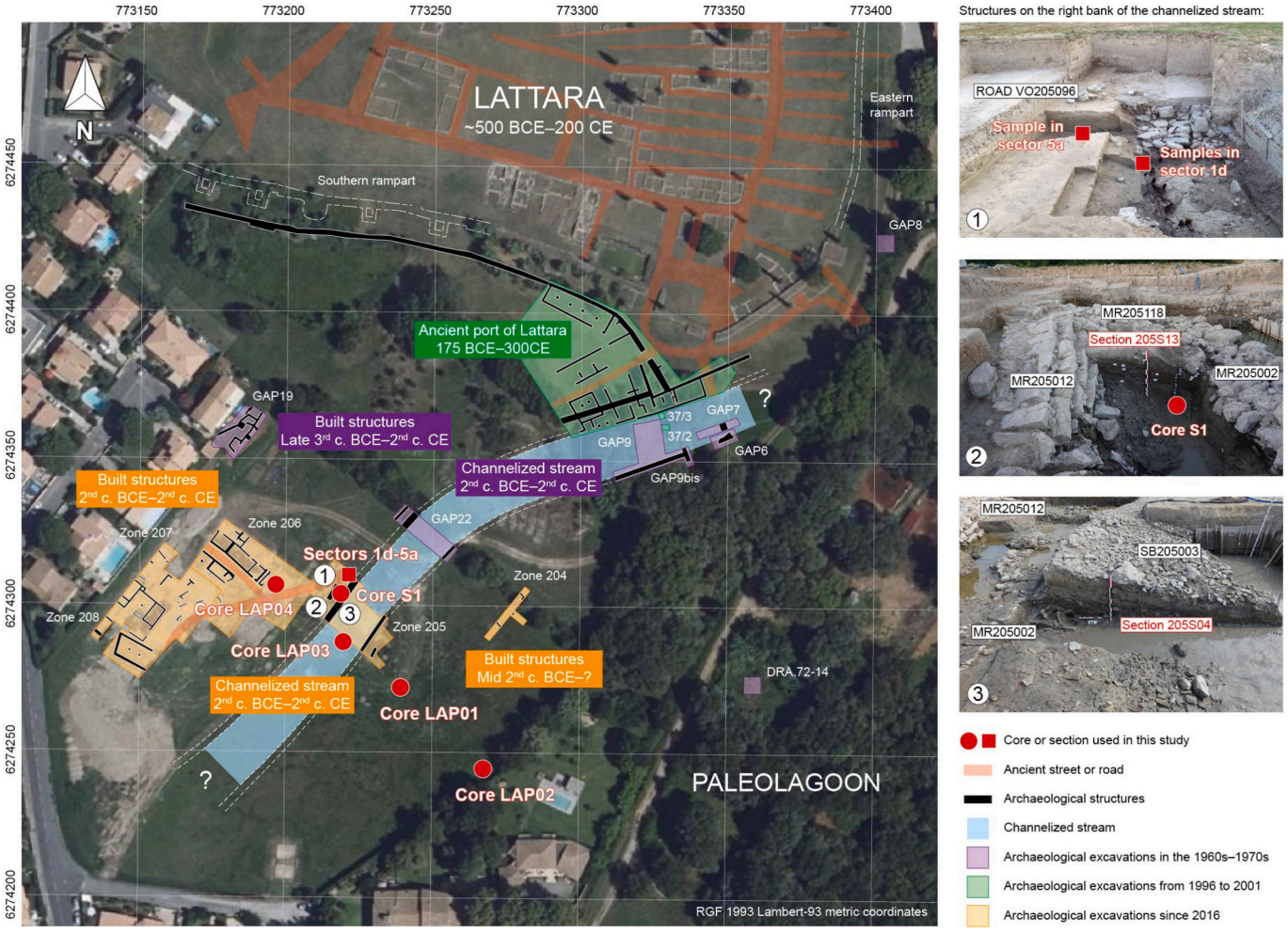

Fig. 2. Harbor facilities south of Lattara and location of cores and samples used in this work. Archaeological data from Arnal et al. (1974), Py (1988, 2009), Garcia and Vallet (2002) and Piquès (2019, 2022). Source of satellite imagery: IGN (www.geoportail.gouv.fr).

3.3. *Particle size analysis*

The particle size distribution (PSD) of 281 sediment samples collected from cores LAP01–04 and sectors 1d-5a at an average resolution of 10 cm was measured from 0.01 to 2000 µm diameter using a Malvern MS3000 laser particle sizer equipped with a 633 nm He-Ne laser source and a hydro LV module set at a stirring speed of 2000 rpm. Refractive and absorption indexes of particles were set at 1.6 and 0.01, respectively. Samples were stirred during 2 h in a 0.5% solution of sodium hexametaphosphate. Obscuration rates ranged between 5 and 30%. Six replicates were measured with a total counting time of 60 s for each sample, and the three replicates with the lowest mean (< 10%) of relative standard deviations of quantiles d_{10}, d_{50} and d_{90} were used to calculate a mean laser PSD. Moreover, 19 samples containing granules (2–4 mm diameter) and fine pebbles (4–8 mm diameter) were measured by sieve analysis in the size range 0.5–8 mm, with the 0.5–2 mm fraction used to combine the two PSD obtained by laser particle sizer and sieving. *C-M* patterns based on median (*M*, d_{50}) and coarsest percentile (*C*, d_{99}) were used to analyze depositional processes (Passega, 1964; Passega and Byramjee, 1969; Arnaud-Fassetta, 2004; Degeai et al., 2022).

3.4. *Magnetic susceptibility*

Magnetic susceptibility (MS) can be used to estimate the oxidation rate of delta plain deposits (Dearing, 1999; Degeai et al., 2020) or terrigenous input into a lagoon (Degeai et al., 2015, 2022). MS measurements were performed with a Bartington MS2 Magnetic Susceptibility Meter and repeated twice for each sample. The mass MS of 281 dried and milled samples collected at a mean resolution of 10 cm in cores LAP01–04 and sectors 1d-5a was measured by a MS2B sensor at a frequency of 4.65 kHz and with a period of 15 s. The relative standard deviation of duplicates was lower than 5%. The volume MS of core S1 was measured at 5-cm resolution by a MS2F probe at a frequency of 0.58 kHz and with a period of 1.1 s.

3.5. *Molluscs*

Mollusc shells were collected in the >0.5 mm fraction of 274 samples from cores LAP01–04 and S1 and in the >1 mm fraction of 3 samples from sectors 1d-5a. A total of 94 taxa were identified under a stereomicroscope and assigned to five ecological habitats (terrestrial, freshwater, supralittoral, midlittoral and sublittoral) according to D'Angelo and Gargiullo (1978), Clanzig (1987), Glöer and Meier-Brook (1998), Kerney and Cameron (2006), Garmony and Ripken (2011), Welter-Schultes (2012), Giaime et al. (2017) and La Rivière et al. (2021) (Table S1). The number of valves was divided by 2 for bivalve species. The number of opercula of *Bithynia tentaculata* and *Pomatias elegans* was taken into account if it was greater than the number of shells of each of these species. Burrowing species such as *Ceciloides acicula* were excluded from relative counts.

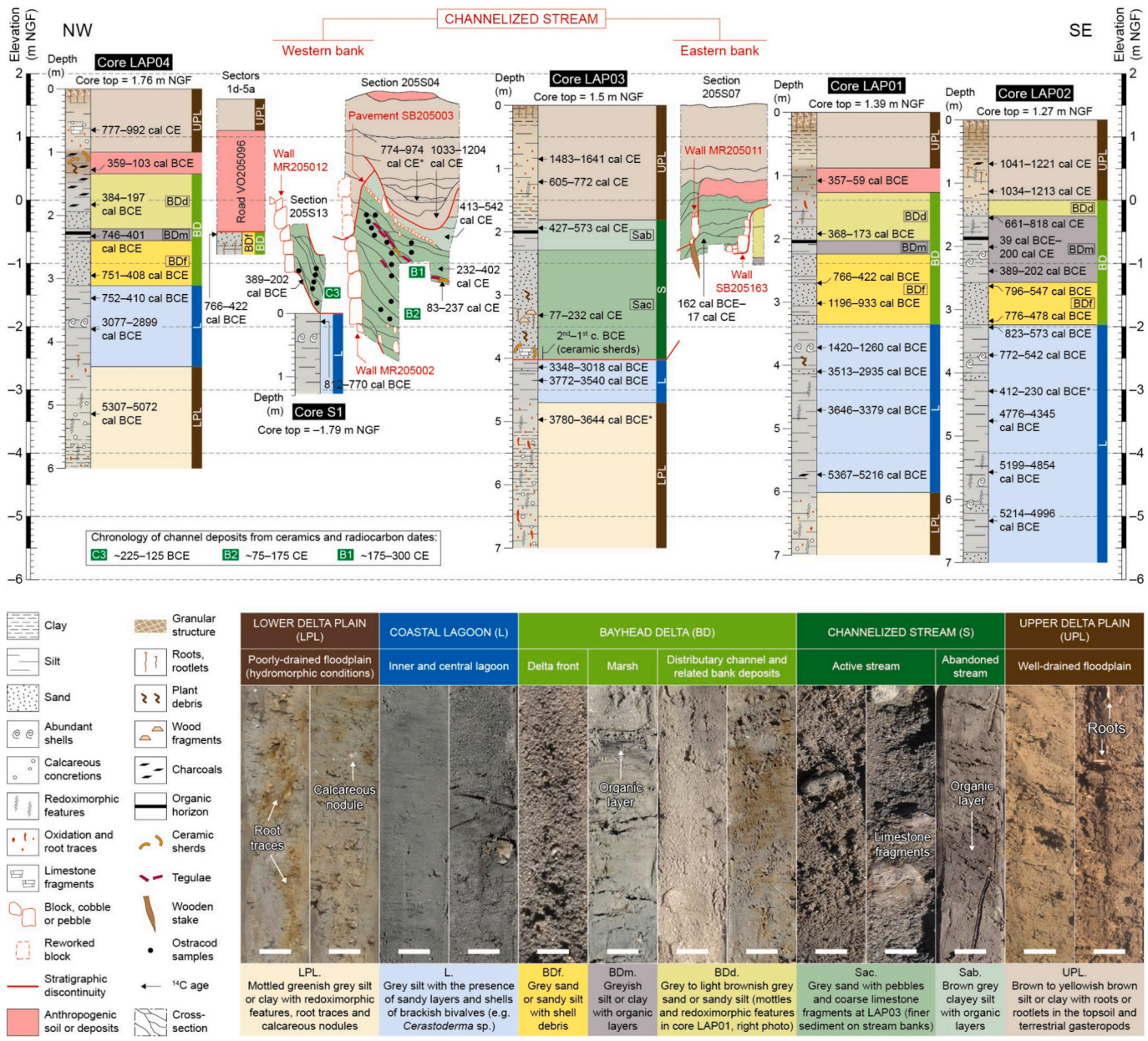

Fig. 3. Chronology and sedimentary facies of Holocene deposits south of Lattara. Ceramic chronology of deposits C3, B2 and B1 from Piquès (2019, 2022). White scale bar on pictures: 2 cm. Radiocarbon dates with an asterisk are not consistent and excluded from age models. NGF: Nivellement Général de la France (French Geodetic Datum).

3.6. Ostracods

The ostracod fauna of 53 samples was studied using stereomicroscopic observations and scanning electronic microscope images (Fig. S1) in order to estimate the salinity range of aquatic ecosystems. Ostracods were collected in the >125 µm fraction of samples from cores LAP01–04. The coarse deposits in the middle part of core LAP03 were barren of ostracods, therefore we have used the >200 µm fraction of samples collected for bioarchaeological studies in sections 205S04 and 205S13 (Fig. 3) to characterize the paleosalinity in the channelized stream. A minimum of 100 valves were counted apart from samples with very low abundances. 28 taxa identified according to Bonaduce et al. (1975), Oertli (1985), Athersuch et al. (1989), Meisch (2000) and Fuhrmann (2013) were classified into five categories of salinity from Salel et al. (2016, 2019): limnetic to mesohaline (<18‰), oligohaline to hyperhaline (0.5–150‰), oligohaline to euhaline (0.5–40‰), mesohaline to euhaline (5–40‰) and polyhaline to euhaline (18–40‰) (Table S2).

3.7. Macrocharcoal counting

An increase in the abundance of charcoals in sediment combined with relatively higher MS values can indicate an increased fire activity (e.g. Patterson et al., 1987; Millspaugh and Whitlock, 1995; Zielhofer et al., 2010). Coarse charcoals are representative of local fires rather than regional fires (Whitlock and Larsen, 2001; Vachula et al., 2018). Local fires around the archaeological site of Lattara can be detected by counting the number of macrocharcoals in the >500 µm fraction of 286 samples from cores LAP01–04 and S1. Macrocharcoal concentration (in macrocharcoals•cm^{-3}) was multiplied by sediment accumulation rates (SAR, in cm•yr^{-1}) to calculate macrocharcoal accumulation rates (in macrocharcoals•cm^{-2}•yr^{-1}).

Table 1
AMS radiocarbon dates in sediments south of Lattara.

Core or section (depth in cm)	Altitude in m NGF	Material	Laboratory code	Radiocarbon age in BP	2 sigma age range (median probability)
LAP01 (100–116)	0.31	Charcoal	Poz-136373	2165 ± 30	357–59 cal BCE (−215)
LAP01 (191–192)	−0.53	Charcoal	Poz-116872	2200 ± 30	368–173 cal BCE (−280)
LAP01 (269–270)	−1.31	Plant debris	Poz-116873	2470 ± 30	766–422 cal BCE (−625)
LAP01 (301−302)	−1.63	Charcoal	Poz-116970	2880 ± 30	1196–933 cal BCE (−1060)
LAP01 (377–368)	−2.33	Charcoal	Poz-136290	3075 ± 30	1420–1260 cal BCE (−1340)
LAP01 (414–406)	−2.71	Charcoal	Poz-148312	4540 ± 80	3513–2935 cal BCE (−3225)
LAP01 (478–464)	−3.32	Charcoal	Poz-116874	4780 ± 50	3646–3379 cal BCE (−3565)
LAP01 (575–570)	−4.34	Charcoal	Poz-116876	6325 ± 35	5367–5216 cal BCE (−5295)
LAP02 (75–64)	0.57	Charcoal	Poz-148032	895 ± 35	1041–1221 cal CE (1155)
LAP02 (117–108)	0.14	Seed	Poz-136293	920 ± 40	1034–1213 cal CE (1115)
LAP02 (164–147)	−0.28	Seed	Poz-148033	1285 ± 30	661–818 cal CE (725)
LAP02 (200−201)	−0.74	Seed	Poz-121287	1955 ± 30	39 cal BCE–200 cal CE (70)
LAP02 (245–234)	−1.12	Charcoal	Poz-148034	2240 ± 30	389–202 cal BCE (−280)
LAP02 (269–257)	−1.36	Wood	Poz-136294	2540 ± 30	796–547 cal BCE (−600)
LAP02 (324–312)	−1.91	Plant debris	Poz-136295	2490 ± 35	776–478 cal BCE (−635)
LAP02 (333–324)	−2.01	Charcoal	Poz-148035	2595 ± 35	823–573 cal BCE (−700)
LAP02 (376–368)	−2.45	Charcoal	D-AMS 053415	2494 ± 23	772–542 cal BCE (−745)
LAP02 (435–424)	−3.02	Charcoal	Poz-148156	2310 ± 30	412–230 cal BCE (−385)
LAP02 (484–469)	−3.49	Charcoal	Poz-136375	5690 ± 100	4775–4345 cal BCE (−4540)
LAP02 (561–552)	−4.3	Charcoal	D-AMS 053414	6074 ± 26	5199–4854 cal BCE (−4980)
LAP02 (640–630)	−5.08	Charcoal	Poz-120418	6160 ± 40	5214–4996 cal BCE (−5110)
LAP03 (80–90)	0.65	Charcoal	Poz-121288	325 ± 30	1483–1641 cal CE (1560)
LAP03 (130−113)	0.29	Charcoal	Poz-148157	1370 ± 30	605–772 cal CE (655)
LAP03 (198–190)	−0.44	Seed	Poz-121290	1560 ± 30	427–573 cal CE (495)
LAP03 (331−332)	−1.82	Wood	Poz-120578	1890 ± 30	77–232 cal CE (155)
LAP03 (416–411)	−2.64	Plant debris	Poz-157791	4470 ± 40	3348–3018 cal BCE (−3190)
LAP03 (440–431)	−2.85	Plant debris	Poz-121741	4890 ± 40	3772–3540 cal BCE (−3680)
LAP03 (504–490)	−3.47	Plant debris	Poz-136420	4935 ± 35	3780–3644 cal BCE (−3700)
LAP04 (60–70)	1.11	Seed	D-AMS 044262	1123 ± 24	777–992 cal CE (935)
LAP04 (127–128)	0.48	Charcoal	Poz-135795	2170 ± 30	359–103 cal BCE (−230)
LAP04 (182–183)	−0.07	Charcoal	Poz-136421	2220 ± 30	384–197 cal BCE (−280)
LAP04 (240–225)	−0.57	Charcoal	Poz-148158	2415 ± 30	746–401 cal BCE (−490)
LAP04 (299–291)	−1.19	Charcoal	Poz-148159	2440 ± 30	751–408 cal BCE (−535)
LAP04 (336–326)	−1.55	Charcoal	Poz-148014	2445 ± 30	752–410 cal BCE (−550)
LAP04 (379–380)	−2.04	Charcoal	Poz-136422	4350 ± 30	3077–2899 cal BCE (−2965)
LAP04 (519–508)	−3.38	Seed	D-AMS 044263	6247 ± 30	5307–5072 cal BCE (−5245)
S1 (102−110)	−1.92	Charcoal	D-AMS 044260	2604 ± 28	812–770 cal BCE (−795)
Sector 5a (0–8)	−0.54	Charcoal	Poz-157793	2470 ± 30	766–422 cal BCE (−625)
205S04, US205046	ca. 0	Seed	Poz-116876	1170 ± 30	774–974 cal CE (860)
205S04, US205048	ca. –0.3	Charcoal	Poz-167348	925 ± 30	1033–1204 cal CE (1105)
205S04, US205049	ca. –0.6	Seed	Poz-167707	1610 ± 30	413–542 cal CE (475)
205S04, US205035	ca. –1	Plant debris	Poz-162076	1760 ± 35	232–402 cal CE (305)
205S04, US205038	ca. –1.3	Seed	Poz-161604	1875 ± 30	83–237 cal CE (170)
205S07, US205124	ca. –0.6	Seed	Poz-116960	2060 ± 30	162 cal BCE–17 cal CE (−70)
205S13, US205354	ca. –1.2	Wood	Poz-120579	2240 ± 30	389–202 cal BCE (−280)

4. Results

4.1. Chronology and depositional environment

4.1.1. Lower delta plain (LPL)

The lower delta plain is composed of mottled greenish grey silt or clay showing redoximorphic features, calcareous nodules, oxidation and root traces below ca. 4.4, 4.7 and 6 m depth in cores LAP04, LAP03 and LAP01, respectively (Fig. 3). The color of dry powder samples is pale yellow (2.5Y 8/2) from the Munsell chart. These sediments were mainly deposited before 5000 cal BCE. Molluscan shells exhibit relatively high abundances of terrestrial gastropods (main taxa: *Oxyloma elegans*, *Vallonia* sp., *Vertigo Pygmaea*, *Cernuella virgata*, *Monachia cantiana*, *Pomatias elegans*) or freshwater species such as *Bithynia tentaculata* (Fig. 4, Table S1). The low abundance of shells in the lower delta plain could be explained by decalcification and reprecipitation of carbonate, as suggested by the presence of calcareous nodules (Fig. 3).

4.1.2. Coastal lagoon (L)

Lagoonal sediments composed of grey silt intercalated with 5–20 cm thick sand layers were mostly deposited between ca. 5000 and 1000 cal BCE, i.e. in the Neolithic and Bronze Ages. The Munsell color of dry sediment is light grey (2.5Y 7/1) or grey (2.5Y 6/1).

These lagoonal sediments show a decrease and an increase in the relative abundance of shells of terrestrial and brackish-marine species, respectively (Fig. 4). Two subenvironments can be distinguished: an inner lagoon influenced by freshwater input (Li) and a central lagoon with marine influences (Lc). The molluscan and ostracod assemblages of Li are dominated by midlittoral species (*Hydrobia acuta/Ecrobia ventrosa*) and *Cyprideis torosa* with relative mean abundances of 70% in both cases. *C. torosa* is dominant in confined environments along the northwestern Mediterranean coast (Salel et al., 2016). Lc is characterized by a significant increase in the relative abundance of sublittoral molluscs (ca. 40% on average, main taxa: *Cerastoderma* sp., *Abra alba*, *Mytilaster marioni*, *Loripes lacteus*, *Bittium reticulatum*, *Rissoa parva*, *Retusa truncatula*, *Chrysallida obtusa*) and mesohaline or polyhaline to euhaline ostracods (55% on average, taxa: *Xestoleberis* sp., *Loxoconcha rhomboidea*, *Leptocythere* sp., *Callistocythere littoralis*, *Aurila arborescens*), which show a higher tolerance to marine water (Fig. 4, Table S2). A mixture of brackish-marine and continental ostracods such as *Darwinula stevensoni*, *Ilyocypris bradyi/gibba* or *Pseudocandona* cf. *parallela* in the lagoonal deposits from core LAP03 and at the top of Li in core LAP02 seems to indicate the proximity of the delta plain.

The lagoonal sediments L show a southeastward increase in depth and thickness (Fig. 3). The top of these sediments lies between −1 and −2 m NGF in cores LAP04, LAP01 and LAP02.

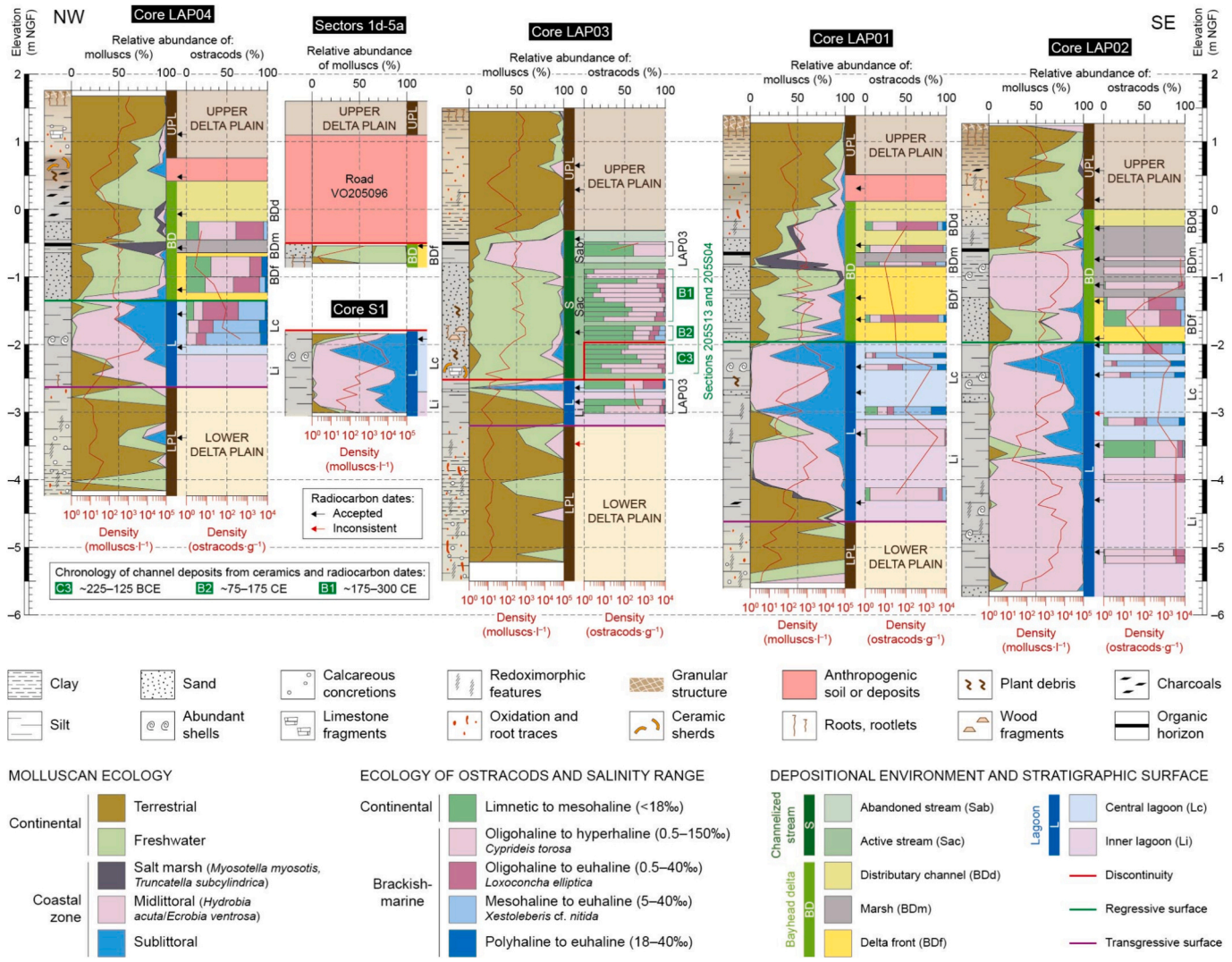

Fig. 4. Molluscan and ostracod biostratigraphy of the sediments south of Lattara. NGF: Nivellement Général de la France (French Geodetic Datum).

4.1.3. Bayhead delta (BD)

The sedimentary facies and bioindicators of the bayhead delta above lagoonal sediments L are related to delta front (BDf), marsh (BDm) or distributary (BDd) subenvironments (Figs. 3–4). The sand of this bayhead delta is mostly composed of reworked carbonate clasts and concretions.

The delta front BDf at the bottom of the bayhead delta is dated between ca. 1200 and 400 cal BCE and corresponds to a 0.7–1 m thick layer of grey sand or sandy silt (Fig. 3). BDf exhibits an increase in the relative abundance of freshwater shells (55% on average, main taxa: *B. tentaculata*, *Valvata* sp., *Belgrandia* sp., *Planorbis planorbis*) and continental or oligohaline to hyperhaline/euhaline ostracods (90% on average, main taxa: *D. stevensoni*, *I. bradyi/gibba*, *C. torosa*, *L. elliptica*) indicating the existence of a river mouth (Salel et al., 2016), whereas the presence of sublittoral molluscs along with polyhaline to euhaline ostracods such as *Leptocythere* sp. and *Callistocythere* sp. is an evidence of marine influence (Fig. 4).

Marsh deposits (BDd) may be intercalated between the delta front BDf and distributary channel BDd. These are composed of greyish silt or clay with organic layers deposited around 500 cal BCE at LAP01 and LAP04, and between 500 cal BCE and 800 cal CE at LAP02 (Fig. 3). BDm is generally characterized by monospecific populations of *H. acuta/E. ventrosa* and *C. torosa* at LAP02 or by relatively high abundances of *C. torosa* (>50%) and supralittoral species (*Myosotella myosotis* and *Truncatella subcylindrica*, ca. 50% on average) at LAP01 and LAP04 (Fig. 4). Besides, a drastic increase in the relative abundance of freshwater and terrestrial molluscs above −0.6 m NGF at LAP02 reveals the transition from a brackish to a slightly brackish-freshwater marsh.

The distributary channel BDd in the upper part of the bayhead delta is composed of grey to light brownish grey sand or sandy silt deposited around 400–200 cal BCE at LAP01 and LAP04, and around 800–1000 cal CE at LAP02 (Fig. 3). Sandy silt contains charcoals at LAP04 and shows orange mottles and redoximorphic features at LAP01. The ostracod assemblages of BDd show high relative abundances of L. *elliptica* and *C. torosa* (45 and 40% on average, respectively) and the minor presence of continental and mesohaline/polyhaline to euhaline ostracods, while the molluscan assemblages are characterized by the dominance of terrestrial and freshwater molluscs (80% on average) apart from core LAP01 represented by a mix of continental and coastal species (Fig. 4). Besides, the continental ostracods of this bayhead delta were partially reworked.

A 50 cm thick dark brown or dark grey anthropogenic soil dated at ca. 360–100 and 360–60 cal BCE overlies the bayhead delta in cores LAP04 and LAP01, respectively (Fig. 3). This anthropogenic soil contains ceramic sherds, plant debris and charcoals at LAP04.

4.1.4. Channelized stream (S)

The sediments of the channelized stream between LAP04 and LAP01 are dated between ca. 200 cal BCE and 400 cal CE (Fig. 3). These sediments are composed of grey carbonate sand and granules with fine rounded limestone pebbles between 4 and 2.3 m depth in core LAP03 (active stream Sac), while finer deposits mainly composed of silt and sand are present along the stream banks in sections 205S13 and 205S04. The lower part of Sac in core LAP03 contains coarse limestone fragments along with ceramic sherds dating from the 2nd–1st centuries BCE, and overlies lagoonal sediments L dated around 3500–3000 cal BCE, which highlights a sedimentary hiatus of about 3000 years. The molluscan shells in the coarse deposits Sac correspond mainly to freshwater taxa such as *B. tentaculata*, *Belgrandia* sp. and *T. fluviatilis* (Fig. 4). The ostracod fauna of the sediments deposited along the stream banks (sections 20513 and 205S04) is primarily composed of *C. torosa* and continental ostracods such as *Candona angulata*, *D. stevensoni*, *Heterocypris salina* and *I. bradyi/gibba*, with mean relative abundances of 50 and 40%, respectively.

The top of the channelized stream S in core LAP03 corresponds to the fine sediments of an abandoned stream (Sab) composed of brown grey clayey silt with organic layers deposited between ca. 400–600 cal CE, i.e. in Late Antiquity and the Early Middle Ages (Fig. 3). Brackish to freshwater conditions prevailed in Sab (Fig. 4), as suggested by relatively high abundances of *H. acuta/E. ventrosa* and freshwater molluscs (50 and 35% on average, respectively), and by a balanced distribution of *C. torosa* (50% on average) and continental ostracods such as *H. salina* (20–50%) and *I. bradyi/gibba* (10–50%).

4.1.5. Upper delta plain (UPL)

The upper delta plain corresponds to a ca. 1–2 m thick layer of brown to yellowish brown clay or silt with terrestrial gastropods mostly deposited in the last millennia (Fig. 3). The Munsell color of dry sediment is pale yellow (2.5Y 7/3 or 2.5Y 8/2). Modern soils at the top of cores generally show a granular structure with many roots and rootlets. The molluscan fauna of UPL is mainly composed of land snails such as *Cochlicella* sp., *Vallonia* sp., *C. virgata*, *V. pygmaea* and *Succinella oblonga* at LAP04, LAP03 and LAP01, while a more humid environment characterized by a mix of terrestrial and freshwater molluscs prevailed at LAP02 (Fig. 4).

4.2. Depositional processes

Silt and clay in the lower delta plain (LPL) were predominantly transported in suspension (Fig. 5). More specifically, suspended clay was deposited between ca. 6 and 5.5 m depth in cores LAP03–LAP04. Sand content and injection of saltating particles into the suspended load are higher in the direction of core LAP04, which could indicate the proximity of a river channel northwest of the study area.

The lagoonal sediments L are mainly composed of silt deposited from suspension frequently mixed with saltating particles, as in core LAP04, at ca. 5.4–5 and 4.1–3.4 m depth in core LAP01, and at ca. 7–6.6, 6.2–5.2 and 4–3.2 m depth in core LAP02. The sand layers at 6.2–6.1 m depth in core LAP02 and around 4.2 m depth in core LAP03 were probably transported during flood events by suspension, saltation and rolling or by rolling and saltation, respectively.

The delta front deposits (BDf) are composed of either silty sand and sandy silt mainly transported in suspension and by saltation, or of

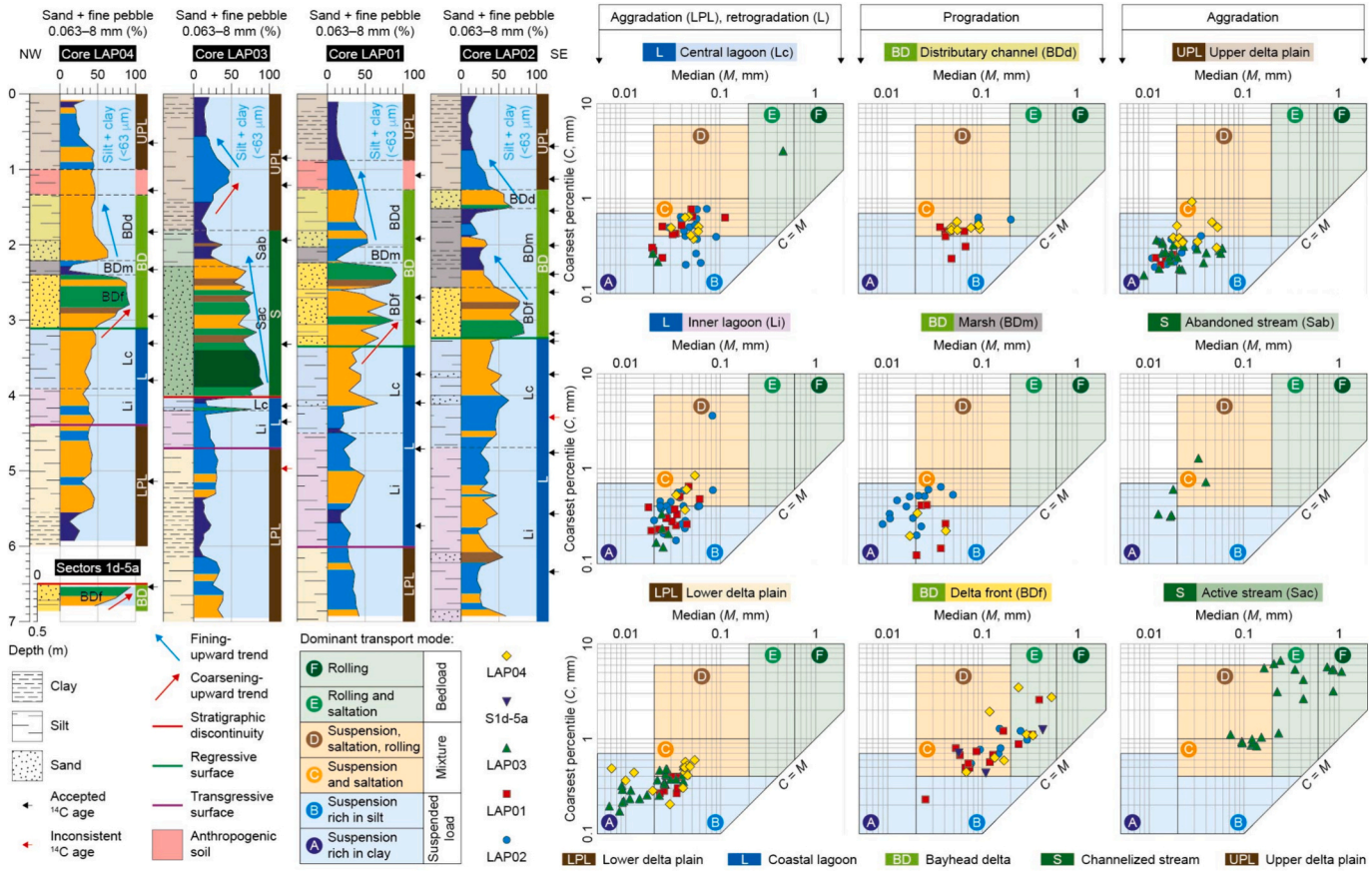

Fig. 5. Grain size and depositional processes of the sediments south of Lattara. Limits of dominant transport modes on *C-M* patterns modified from Passega (1964), Passega and Byramjee (1969) and Arnaud-Fassetta (2004).

coarser sediment containing >80% of sand and fine pebble transported by rolling and saltation. The base of BDf shows a coarsening-upward trend at LAP04, LAP01 and sectors 1d-5a. The transition between the delta front BDf and marsh BDm is characterized by either a drastic decrease in sand content at LAP04 and LAP01 or a fining-upward trend at LAP02. Silt or clay suspension was the dominant mode of sediment transport in the marsh BDm. The distributary channel deposits (BDd) exhibit a fining-upward trend and are mainly composed of a mixture of suspended and saltating particles.

The coarse sediments of the channelized stream in core LAP03 (Sac) also show a fining-upward trend. Rolling was the dominant mode of transport of sand and pebble deposited between 4 and 3.4 m depth, whereas the overlying sediments between 3.4 and 2.3 m depth are composed of sand mainly transported by saltation along with rolling and/or suspension. Suspended sediment occasionally mixed with saltating particles were then deposited at the top of the channelized stream (Sab).

The upper delta plain (UPL) is composed of particles transported only in suspension rich in clay or silt at LAP01–03, while sediments at LAP04 were almost exclusively deposited from silty suspension sometimes mixed with saltating particles. This is coherent with the fact that the Lez River and its tributaries flowed west of the study area over the past millennia (Fig. 1B). Besides, coarse suspension containing from 20 to 50% of sand led to the deposition of silt during the medieval period in the middle part and the lower half of UPL at LAP03 and LAP02, respectively.

4.3. *Terrigenous sediment*

Sediments are mainly composed of diamagnetic or weakly paramagnetic materials with MS values ranging between ca. 0 and $35 \bullet 10^{-8}$ $m^3 \bullet kg^{-1}$ (Fig. 6A). High MS values are generally related to higher abundances of terrestrial molluscs, such as in the lower and upper delta plain (LPL and UPL, respectively) where subaerial deposits were more oxidized. This is coherent with oxidation along root traces in LPL and with brown to yellowish brown sediment color in UPL (Fig. 3), while the formation of modern soils in the upper 30–40 cm of cores LAP01–LAP04 caused a sharp MS increase between 15 and $25 \bullet 10^{-8}$ $m^{-3} \bullet kg^{-1}$ (Fig. 6A).

MS values higher than $5 \bullet 10^{-8}$ $m^3 \bullet kg^{-1}$ are occasionally found in the aquatic environment of the inner lagoon Li, as in cores LAP04, LAP03, LAP01 and LAP02 at −2.4, −3.2, −4 and − 5 m NGF, respectively. Given that Li was close to the lower delta plain LPL, these MS increases were probably caused by terrigenous input into the inner lagoon. By contrast,

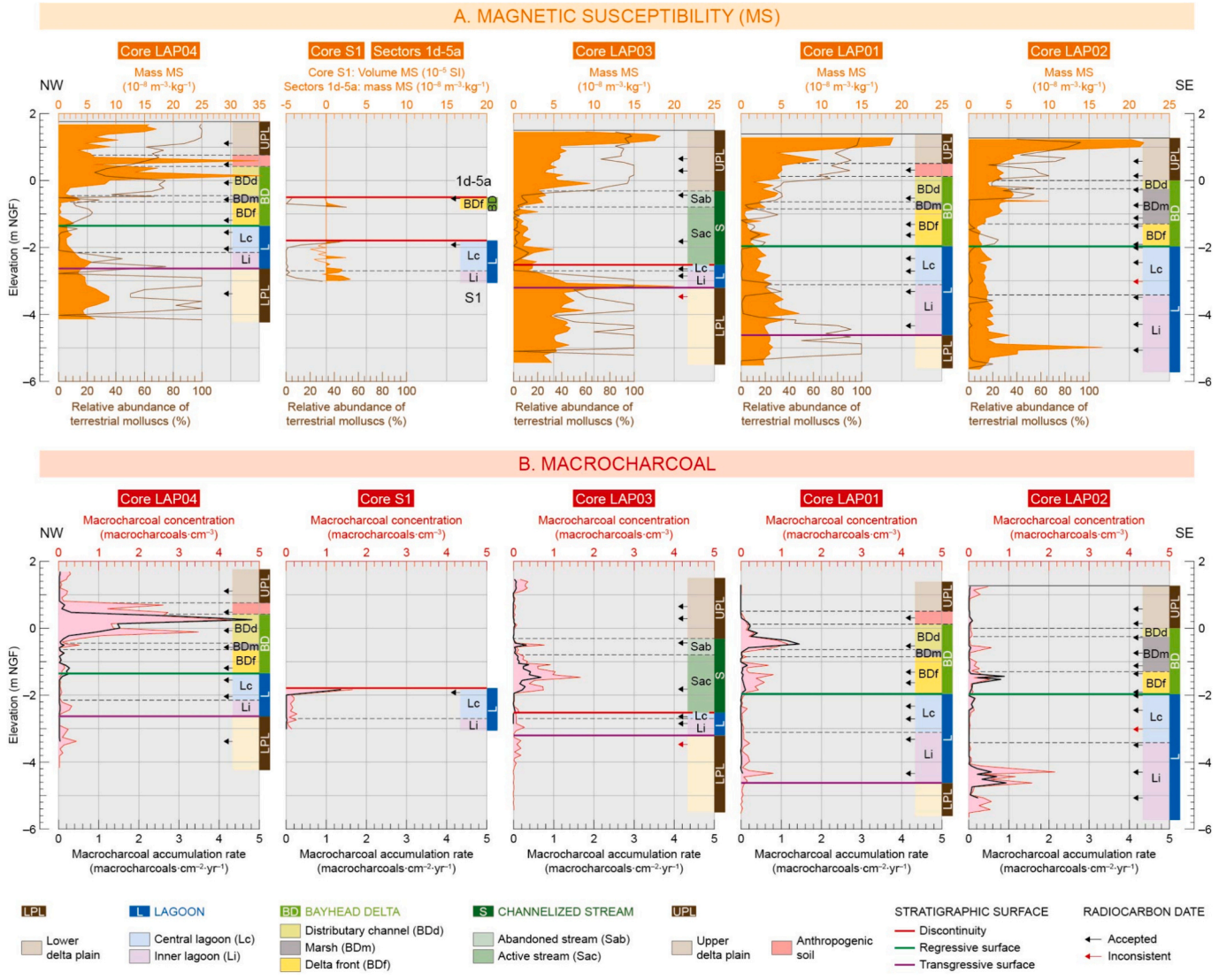

Fig. 6. Magnetic susceptibility and relative abundance of terrestrial molluscs (A) and macrocharcoal concentration and accumulation rate (B) in the sediments south of Lattara. NGF: Nivellement Général de la France (French Geodetic Datum).

the transition from inner to central lagoon was accompanied by a general decrease in MS that suggests a diminution of terrigenous input due to a landward shift of the lagoon shore. Indeed, the sediments of the central lagoon Lc are characterized by low MS values ($<5\bullet10^{-8}$ $m^{-3}\bullet kg^{-1}$) and very low abundances of terrestrial molluscs.

The sands of the delta front BDf and channelized stream S also show MS values below $5\bullet10^{-8}$ $m^{-3}\bullet kg^{-1}$, although riverine inputs and continental influence could have increased from molluscan and ostracod assemblages (Fig. 4). In fact, these sand bodies are predominantly composed of diamagnetic material (carbonates), which could explain abnormally low MS values. The general MS increase in the upper part of the cores LAP01–LAP04 is probably due to the increasing terrestrial influence related to the formation of the distributary BDd and upper delta plain UPL (Fig. 6A). More specifically, the upper half of BDd and the overlying anthropogenic deposits in core LAP04 show high MS values (up to ca. $35\bullet10^{-8}$ $m^3\bullet kg^{-1}$) associated with high concentrations of macrocharcoals (Fig. 6B).

4.4. Macrocharcoal influx

Macrocharcoals are relatively abundant in the middle and upper parts of the distributary BDd at LAP04, with concentrations ranging between 1 and 5 macrocharcoals$\bullet cm^{-3}$ from −0.2 to 0.8 m NGF (Fig. 6B). The highest concentration is found near the top of BDd. The anthropogenic deposits related to the Roman settlement above BDd in core LAP04 also show relatively high concentrations ranging between 1 and 3 macrocharcoals$\bullet cm^{-3}$. The highest accumulation rates of macrocharcoals are found in the upper half of BDd at LAP04, with a maximum value of ca. 5 macrocharcoals$\bullet cm^{-2}\bullet yr^{-1}$ around 0.3 m NGF. The macrocharcoal concentrations and accumulation rates in the lower half of BDd at LAP01 are slightly above 1 macrocharcoal per cm^3 and $cm^2\bullet yr^{-1}$, respectively. Concentrations above 1 macrocharcoal$\bullet cm^{-3}$ are also found around −1.8 m NGF and between −4.6 and − 4.2 m NGF in cores S1 and LAP02, respectively. The deposits of the channelized stream S exhibit a small increase in the concentration and accumulation rate of macrocharcoals between −2 and − 1 m NGF.

5. Discussion

5.1. Sea level changes

Radiocarbon ages and depositional environments identified from molluscan and ostracod assemblages in cores LAP01–LAP04 were used to reconstruct relative sea level (RSL) in the Lez delta plain over the past millennia. Terrestrial (marine) limiting points provide upper (lower) limits on the uncertainty range of RSL (Vacchi et al., 2016; Salel et al., 2020). The past sea level is thus located between these limits. Terrestrial limiting points in the Lez delta include radiocarbon dates from the lower and upper delta plain (LPL and UPL, respectively), as well as those in anthropogenic soils at LAP04 and LAP01 (Fig. 7). Marine limiting points correspond to radiocarbon dates in the lagoonal and delta front deposits (L and BDf, respectively), which are characterized by high abundances

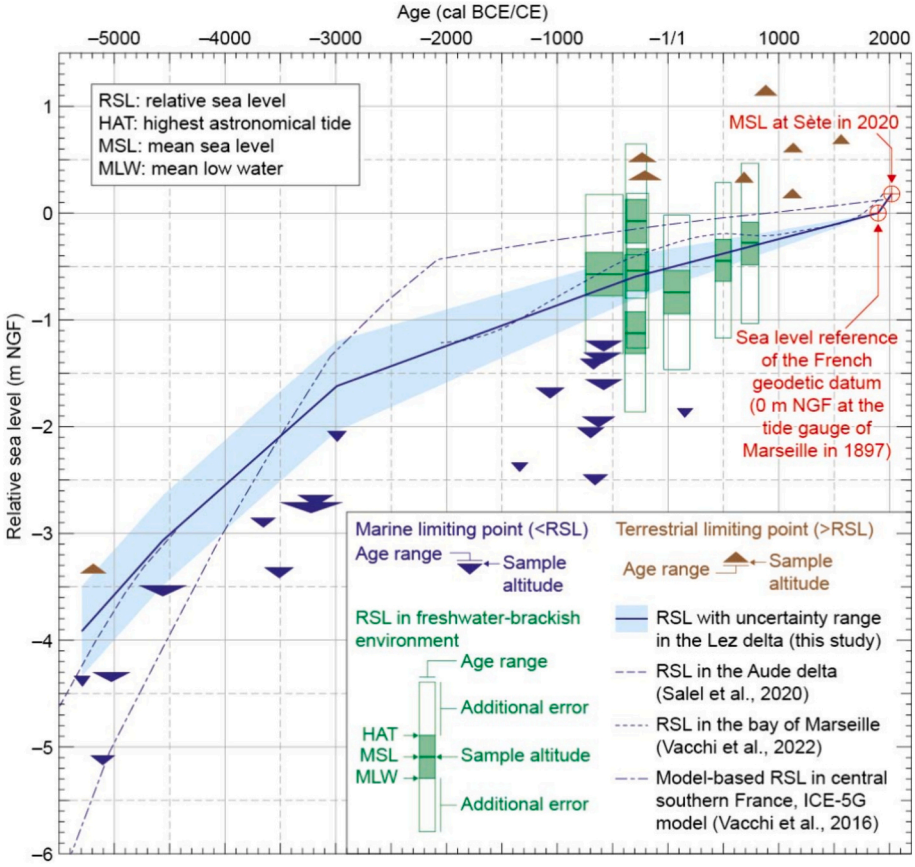

Fig. 7. Relative sea level (RSL) south of Lattara since 5300 cal BCE. The sample altitude of thirty-four radiocarbon ages from cores LAP01–LAP04 (Table 1), sea level reference of the French Geodetic Datum and mean sea level at Sète (Fig. 1A) in 2020 were used to estimate sea level changes. Age range corresponds to the 95.4% probability interval of radiocarbon ages. Additional vertical errors correspond to the root mean square of multiple vertical errors including sample thickness (Table 1), a sampling error of ±0.15 m due to potential core stretching or compaction using a percussion corer, a levelling error of ±0.05 m related to elevation measurement with a differential global positioning system (DGPS), a borehole inclination of 1% for core samples and an environmental uncertainty of ±0.5 m (Vacchi et al., 2016). Sample altitude and RSL are expressed relative to the sea level reference of the French Geodetic Datum (i.e. 0 m NGF in 1897 at the tide gauge of Marseille, see location in Fig. 1A). NGF: Nivellement Général de la France (French Geodetic Datum).

of brackish-marine ostracods (Fig. 4). The radiocarbon age around −1.8 m NGF in the lower part of the channelized stream S at LAP03 is also considered as a marine limiting point under RSL.

Moreover, Vacchi et al. (2016) suggested that RSL ranges between the highest astronomical tide (HAT) and mean low water (MLW) in environments characterized by micro- and macrofossil assemblages dominated by freshwater-brackish to shallow marine taxa. These conditions are found in marsh (BDm) and distributary (BDd) subenvironments, as well as at the top of the channelized stream (Sab). In this case the sample altitude of radiocarbon ages corresponds to the mid-point between HAT and MLW (Vacchi et al., 2016). HAT (MLW) in the Lez delta can be estimated around 0.2 m above (below) mean sea level from tide gauge data of the Service Hydrographique et Océanographique de la Marine (SHOM) at Sète (Fig. 1A, data available at https://doi.org/10.17183/refmar#250). Vertical errors were added to this RSL range (Fig. 7).

It is probable that Holocene sea level changes in the coastal area of the Lez River were not controlled by tectonics, given that the area between Lattes and Narbonne (Fig. 1A) seems to have been tectonically stable over the past 500,000 years (Ambert, 1999; Degeai, 2021). RSL in the Lez River delta is estimated to be between −4.3 and − 3.4 m NGF around 5200 cal BCE (Fig. 7), which is consistent with RSL reconstructed in the Aude River delta near Narbonne by Salel et al. (2020). Besides, Vacchi et al. (2016) proposed a model-based reconstruction of RSL changes in central southern France using the ICE-5G Glacial Isostatic Adjustement (GIA) model and a large dataset of sea-level index points between Sète and Fréjus (Fig. 1A). The nominal RSL curve predicted by this model shows lower (higher) values before (after) 3500 cal BCE compared to mean our RSL estimates (Fig. 7).

RSL in the Lez delta system is estimated at −0.6 ± 0.2 m NGF around 200 cal BCE. This agrees with the lowest elevation of the road VO205096 along the western bank of the channelized stream S (Figs. 2–3), which was found to be around −0.5 m NGF at this time (Piquès, 2022). A mean RSL of −0.5 m NGF can be proposed for the transition between the 1st century BCE and the 1st century CE (Fig. 7), during which the mean water level in a coastal lagoon south of Narbonne was estimated between −0.6 and − 0.3 m NGF (Flaux et al., 2020). Otherwise, the mean RSL reconstructed by Vacchi et al. (2016) from marine notches in the bay of Marseille (Fig. 1A) over the past 4000 years is mostly in the uncertainty range of RSL estimated for the Lez delta plain, except for the first half of the first millennium CE during which the former is slightly above the latter (Fig. 7).

5.2. *Delta architecture*

Age-depth models coupled to sea level reconstructions and palaeoenvironmental data can be used to study the geomorphic and stratigraphic setting of ancient harbors in deltaic environments (Salomon et al., 2016). The aggradation of the lower delta plain LPL south of Lattara was followed by a lagoonal transgression in a context of relatively rapid sea level rise (Fig. 8), which may have caused flooding of coastal plains (Catuneanu et al., 2011). The lower delta plain LPL is poorly drained and shows redoximorphic features and calcareous nodules (Fig. 3), which suggest a depositional environment characterized by frequent floods interspersed with brief episodes of subaerial exposure (Amorosi et al., 2013a). The lagoonal transgression occurred locally at LAP04 around 4000 cal BCE. A retrogradational stacking pattern is associated with the lagoonal sediments overlying the transgressive surface visible in cores LAP04, LAP03 and LAP01 (Figs. 8, 9A). The transition from inner to central lagoon that occurred between 4200 and 3200 cal BCE from southeast to northwest was accompanied by a decrease in sediment accumulation rates and an increase in water depth and accommodation space (Fig. 8). The top of lagoonal sediments Lc corresponds to a regressive surface covered by prograding sand bodies in cores LAP04, LAP01 and LAP02.

The coalescence and amalgamation of mouth bar sands has probably contributed to the formation of the delta front at the bottom of the bayhead delta (Amorosi et al., 2013b, 2017; Ponce et al., 2024). Delta front and mouth bars are formed in the lower part of the bayhead delta below sea level (Chamberlain et al., 2018). Proximal to medial delta front consists of mouth bars associated with terminal distributary channels (Bhattacharya, n.d.; Aschoff et al., 2018). The distal margins of

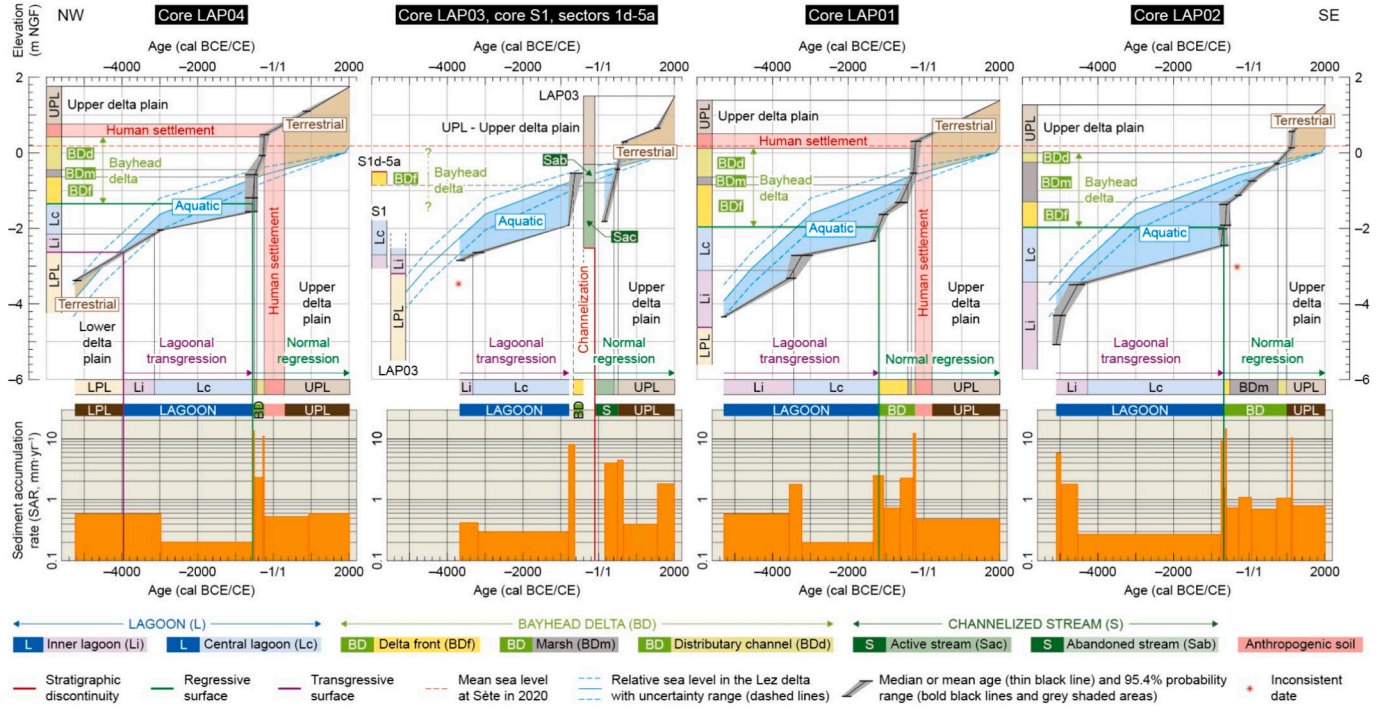

Fig. 8. Depositional environments, age models, relative sea level and sediment accumulation rates south of Lattara. NGF: Nivellement Général de la France (French Geodetic Datum).

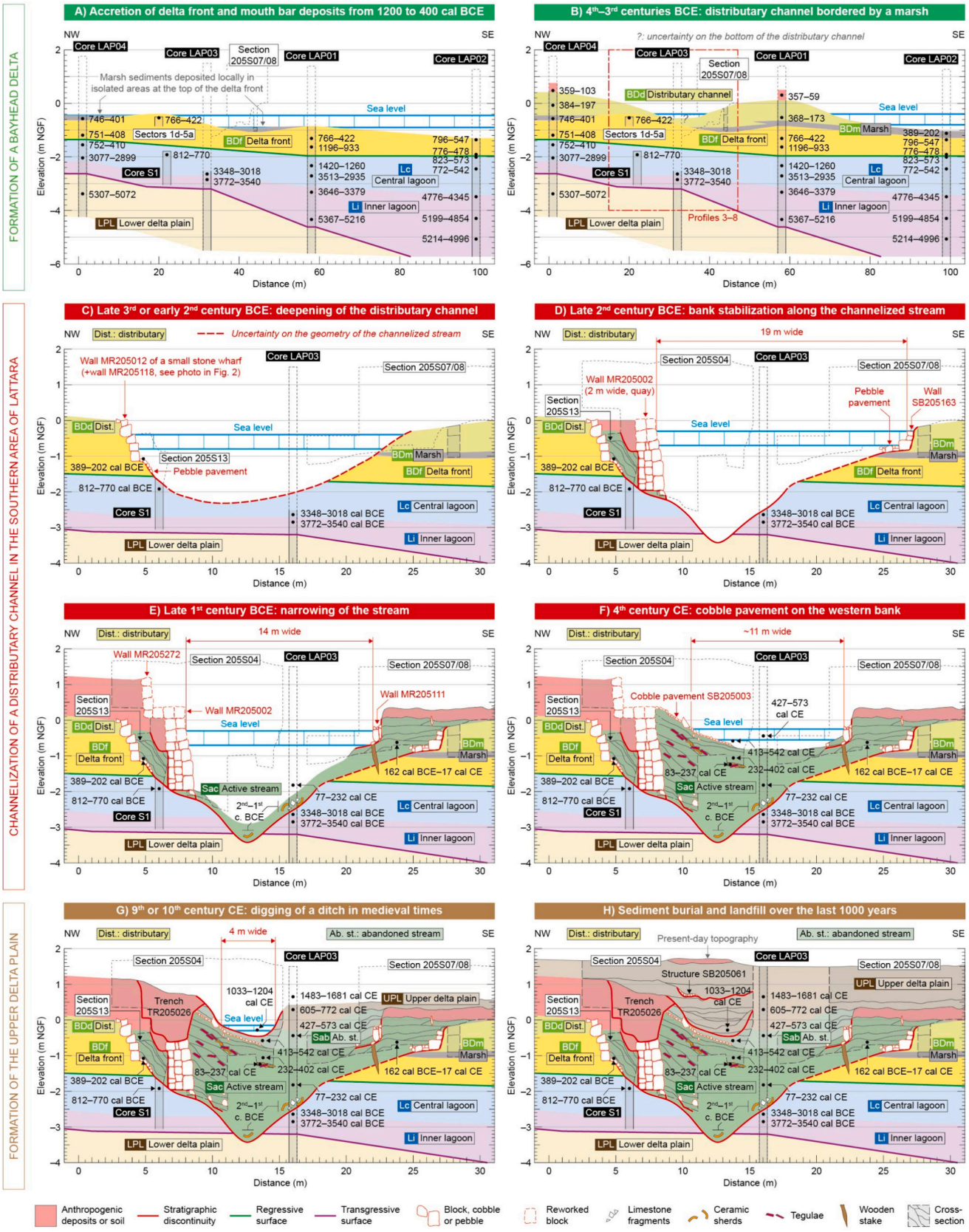

Fig. 9. Geomorphic evolution before, during and after the channelization of a distributary channel south of Lattara. Black dot: radiocarbon age with 95.4% probability interval. Blue lines: uncertainty range of sea level from estimates in Fig. 7. NGF: Nivellement Général de la France (French Geodetic Datum). (For interpretation of the references to color in this figure legend, the reader is referred to the web version of this article.) (For interpretation of the references to color in this figure legend, the reader is referred to the web version of this article.)

these bars are commonly formed by frontal splays interbedded with finer sediments, which can be considered as a distal delta front (Bhattacharya, n.d.; Ahmed et al., 2014).

In the case of the Lez delta, the succession of sandy silt and silt between ca. 3.6 and 2.4 m depth at LAP01 (Fig. 5) can be associated with a distal delta front formed in the earliest phase of progradation between 1200 and 800 cal BCE, then the widespread deposition of mouth bar sands between 800 and 400 cal BCE from LAP04 to LAP02 would be related to a proximal delta front close to the distributary channel. Sharp increases in SAR coupled to a decreasing rate of sea level rise caused a reduction of accommodation space during the formation of the delta front (Fig. 8). The top of the delta front would have been close to sea level in the western part of the study area at the end of this step, which could have led to the local deposition of fine sediments with organic-rich layers in marshes partially or totally isolated from sediment flux and streamflow, as those in core LAP04 or a trench at the bottom of section 205S07/08 (Fig. 9A).

The upper part of a bayhead delta above the delta front and mouth bars is composed of subaerial distributary deposits somewhat organic and finer near their base (Chamberlain et al., 2018). Besides, bedsets of distributary channels fine upward (Aschoff et al., 2018). These features are found in the upper half of the bayhead delta at LAP01, LAP02 and LAP04, where fine sediments with organic layers (BDm) are covered by distributary channel deposits (BDd) showing fining-upward trends and increasing abundance of terrestrial molluscs (Figs. 3–5). The formation of the distributary channel between LAP04 and LAP01 occurred in the 4th and 3rd centuries BCE (Fig. 9B). The eastern side of this distributary channel was bordered by a marsh that persisted until ca. 800 cal CE at LAP02, while the area between LAP04 and LAP01 was characterized by the terrestrial environment of the upper delta plain UPL at this time (Fig. 8). Aggradation with high SAR was the dominant depositional process in the channelized stream from the 2nd century BCE to the 6th century CE.

5.3. Channel, channelized stream or canal?

Ships sailing in deltaic areas may use natural waterways such as river channels, distributaries or coastal lakes, or artificial waterways such as canals. Channelization of river channels was used by the Romans to improve navigation (Arnaud-Fassetta et al., 2003) or to reduce the impact of meandering (Salomon et al., 2023), resulting in channelized streams. It is not always easy to distinguish these different kinds of waterways in ancient harbors, given that the terminology to be used depends on several factors such as geomorphic setting, sediment dynamics, relation to water bodies, as well as archaeological structures or mentions in ancient texts (Salomon et al., 2014a).

Although no historical documentary sources mention the presence of a canal at Lattara in ancient times (Py, 1988), the discovery of architectural elements such as wharf and quay in excavations at Zone 205 (Fig. 2) suggests that ships entered the harbor south of the city (Piquès, 2019, 2020). The ancient waterway south of Lattara was previously interpreted as either a channelized stream of the Lez River (Arnal et al., 1974) or a canal dug along the southern rampart of the city (Py, 1988). Navigation canals as opposed to natural channels may be considered as human-made waterways providing an artificial connection between two water bodies. This does not seem to be the case in the study area where an active distributary channel extending downstream of the paleochannel 2b east of Lattara (Fig. 1B) and connecting the Lez River to Méjean Lagoon already existed before that harbor works were undertaken at the transition between the 3rd and 2nd centuries BCE (9B-C).

A high energy environment was probably associated with the paleochannel 2b at this time, as suggested by the presence of two pebble layers containing protohistoric and Roman ceramic sherds in excavation GAP8 along the eastern rampart of Lattara (Py, 1988) (Fig. 2). Grain size analyses and ostracods assemblages indicate that the distributary channel BDd was active and associated with high energy flow in the 4th and 3rd centuries BCE. Indeed, the *C-M* diagram of deposits BDd (Fig. 5) is similar to those of distributary channels characterized by hydrodynamical conditions typical of high energy environments (Arnaud-Fassetta, 2004), while the mix of brackish and continental ostracods with partial reworking for the latter can be found in distributary channels and river mouths with highly energetic conditions (Amorosi et al., 2009; Salel et al., 2016).

The relatively high bedload concentration in the coarse sediments deposited in the ancient waterway at LAP03 from the 2nd century BCE to the 1st century CE is also indicative of a highly energetic depositional environment (Fig. 10C). Coarse alluvial deposits with high concentrations of bedload may be found in Roman channelized streams, as at the site of Aquileia in northern Italy (Arnaud-Fassetta et al., 2003). However, such deposits may also have been deposited in Roman canals close to river channels during flood events, as at Portus west of Rome (Salomon et al., 2014b).

Furthermore, the geomorphic setting at the time of harbor works in the late 3rd or early 2nd centuries BCE can provide additional information to determine the type of waterway used in ancient times south of Lattara. Archaeological soils and artefacts seem to confirm the presence of an active distributary channel with banks at LAP01 and LAP04 rising above the surrounding areas at the end of the 3rd century BCE, and between which channel water would have flowed before harbor works. The anthropogenic deposits related to the development of urbanization south of Lattara from the late 3rd century BCE overlay the distributary channel deposits at an elevation of 0.4 m NGF at LAP04 and 0.1 m NGF at LAP01 (Fig. 9B). This is on the one hand about 0.3–0.6 m above the archaeological soils composed of pebble pavements from the 2nd-1st centuries BCE discovered in excavations at Zone 206 and GAP19 west of LAP04 (Fig. 2), and on the other hand ca. 1 m above the lagoonal deposits found in excavation DRA.72–14 east of LAP01, which contain Campanian ceramic sherds dated from the late 3rd to the late 1st centuries BCE at Lattara (Py, 1988; Py et al., 2001).

The width of the distributary channel BDd could potentially have reached about 60 m, i.e. the distance between cores LAP01 and LAP04 (Fig. 9B). Besides, it is unlikely that the water depth in this channel exceeded a few decimeters, which was not sufficient for the navigation of deep draught vessels. This may be why the distributary channel was deepened and channelized in several steps from the late 3rd century BCE. Hence, all these observations suggest that the ancient waterway studied in this paper is a channelized stream.

5.4. Water depth in the channelized stream

A small stone wharf (walls MR205012/MR205118) was built on the right bank around 200 cal BCE (Figs. 2, 9C). The width and bottom of this first channelized stream are not precisely known, but RSL estimates and the base of bank deposits covering wall MR205012 in section 205S13 show that its depth exceeded 0.9–1.3 m.

A 2 m wide wall (MR205002) used as a quay on the right bank and a small wall (SB205163) maintaining the left bank were then built in the late 2nd century BCE (Fig. 9D). This resulted in a 19 m wide asymmetric channelized stream with steep slope and higher depth on the right bank in front of the wall MR205002. The water depth in this channelized stream is evaluated at 2.7–3.1 m from the difference between RSL estimates and the stream bottom identified around −3.4 m NGF in an archaeological trench at Zone 205 (Piquès, 2016, 2017). The width and depth of the stream related to this second phase of harbor works were sufficient for the navigation of medium-sized Roman cargo ships such as those encountered in the Rhône delta (Fig. 1A), which may have width and draught at full load of 7.4 and 2.4 m, respectively (Marlier, 2018). However, it was not deep enough for large vessels with 3–3.7 m draught used for maritime transport at this time (Boetto, 2010, 2016).

Channelization undertook by the Romans in the late 1st century BCE led to the enhancement of quay wall MR205002 along with the probable construction of wall MR205272 on the right bank (Piquès, 2020), and to

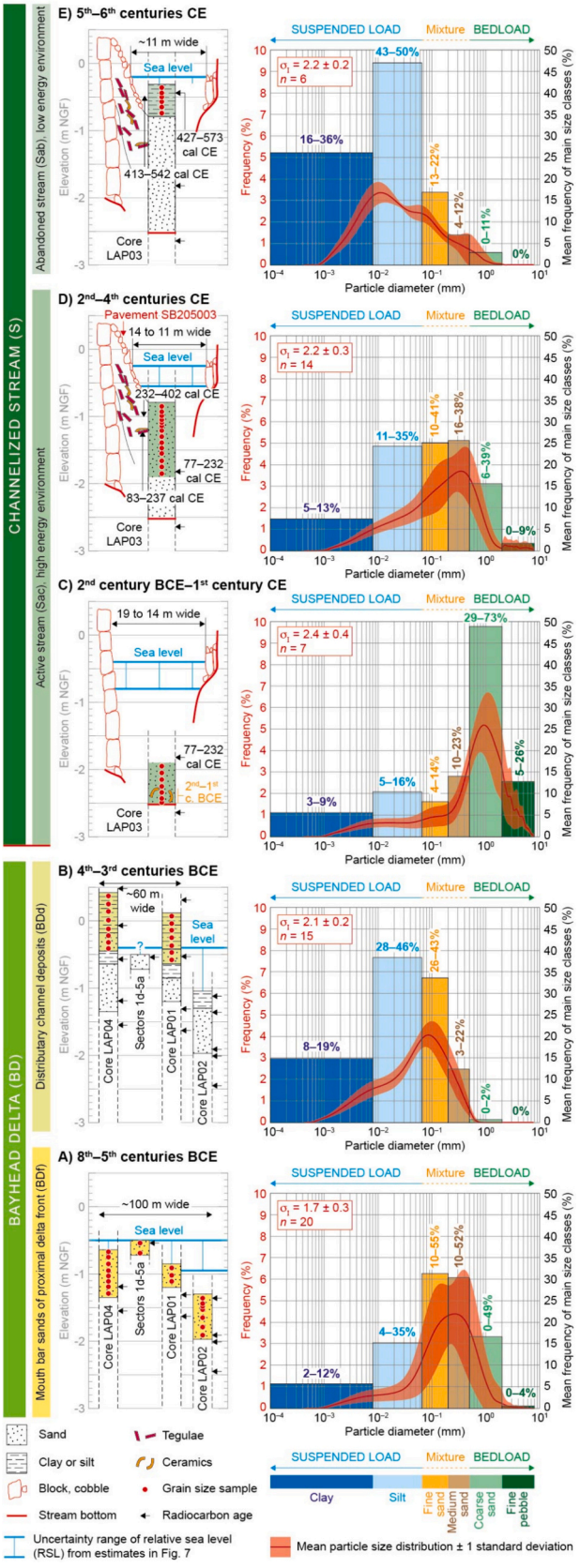

Fig. 10. Evolution of the particle size distributions and depositional processes of the sediments of the bayhead delta and channelized stream south of Lattara. σ_I: mean ± one standard deviation of sorting index from Folk and Ward (1957). *n*: number of samples. NGF: Nivellement Général de la France (French Geodetic Datum).

the construction of wall MR205111 on the left bank (Fig. 9E). This channelization resulted in a 14 m wide stream flanked by anthropogenic deposits (Piquès, 2022).

A cobble pavement (SB205003) was built in the 4th century CE along the right bank of a ca. 11 m wide stream showing a water depth reduced at 0.3–0.6 m (Fig. 9F), which only allowed the navigation of small flat-bottomed barges. Besides, the significant presence of brackish-marine species in all ostracod assemblages of the channelized stream S (sections 205S13 and 205S04, core LAP03) suggests a long-lasting influence of lagoon waters south of Lattara from the first channelization in the late 3rd or early 2nd century BCE to the early Middle Ages (Fig. 4).

Blocks and cobbles of quay MR205002/MR205272 and pavement SB205003 were partially removed by the digging of trench TR205026 on the right bank of the channelized stream in Late Antiquity (Piquès, 2022), then a 4 m wide ditch with a maximal water depth of 0.2–0.3 m was dug in the 9th or 10th century CE (Fig. 9G). RSL estimates suggest that the bottom of this medieval ditch was below sea level at this time. The channelized stream was buried under floodplain deposits of the upper delta plain UPL in the second millennium CE (Fig. 9H). A last shallow ditch of 0.4 m depth was dug in the deposits UPL and covered by a pavement (SB205061) during the modern period.

5.5. *Sediment deposition and channelization*

River channelization and canal digging were undertaken by the Romans in southern Gaul to improve navigation in deltaic areas where mouth bars may have limited the access of deep draft vessels to ancient harbors, as in the Rhône delta (Vella et al., 1999; Rousse et al., 2020), at Narbonne (Sanchez et al., 2016; Faïsse et al., 2018) or Fréjus (Bony et al., 2011) (Fig. 1A). The site of Lattara is particularly interesting because the channelization of a distributary channel was undertaken as soon as the late 3rd century BCE, i.e. approximately one century before the Roman conquest of southern Gaul in the late 2nd century BCE (Christol, 2010). Channelization and harbor works impacted significantly the depositional environments and sediment flux south of Lattara.

Before channelization a minimum width of 100 m between LAP04 and LAP02 was concerned by the deposition of mouth bar sands in the proximal delta front of the bayhead delta from the 8th to the 5th centuries BCE (Fig. 10A). The aggradation and widening of mouth bars were probably controlled by water jet that spreads and decreases downstream the distributary channel as flow progresses basinward from confined to unconfined areas (Edmonds and Slingerland, 2007). Unconfined jet causes a reduction of flow competence (Fagherazzi et al., 2015). In such hydrodynamic conditions the deposition of mouth bar sands south of Lattara was characterized by a mixture of suspended load and bedload composed of ca. 60% of fine to medium sand on average. The mouth bars deposits of the delta front BDf show coarsening-upward trends at LAP04, sectors 1d-5a and LAP01, but a fining-upward trend at LAP02 (Fig. 5). This suggests steeper slope and deeper water at LAP02 (Zhang et al., 2022), which is consistent with RSL estimates and bar depths (Fig. 10A). A minimum width of 60 m between LAP04 and LAP01 was then affected by the deposition of distributary channel sand or silty sand close (BDd) in the 4th and 3rd centuries BCE (Fig. 10B). These deposits were characterized by a relatively more abundant suspended load compared to the mouth bar sands of the proximal delta front (Fig. 10A–B), as well as by a significant increase (decrease) in the mean percentage of silt (medium sand).

Channelization led to a sharp increase in flow competence and sediment flux into a 19 to 14 m wide stream south of Lattara (Fig. 10C). The bottom of the channelized stream in core LAP03 contains an average of ca. 50% of coarse sand deposited as bedload in a high energy environment with relatively higher water depth from the 2nd century BCE to the 1st century CE. River sand and pebble in archaeological trenches GAP6–9 northeast of LAP03 (Fig. 2) were also deposited in a high energy environment at the same time (Arnal et al., 1974; Py, 1988). Stable alluvial channels with high bedload content (35–70%) exhibit width-

depth ratios >25, and streambed aggradation and/or channel widening can occur with lower ratios (Schumm, 1963), which was the case for the channelized stream in the 1st century BCE, with a ratio estimated between 5 and 7 (Fig. 9E). The construction of the walls MR205272 and 205,111 in the late 1st century BCE could have contributed to prevent bank erosion due to natural dynamics of channel widening.

Another potential effect of channelization consists in sediment flushing (De Graauw, 2022; Salomon et al., 2023), especially in high energy environments. This process can evacuate finer particles away from the channelized stream, and one might therefore expect to find well sorted sand in this case. However, the sediments of the channelized stream S as well as those of the mouth bar sands and distributary channel deposits of the bayhead delta BD show sorting index (σ_I) between 1 and 3 (Fig. 10), indicating poor to very poor sorting from the classification of Blott and Pye (2001). Poor sorting may be due to irregular flow occasionally affected by river floods or runoff events (Jorda, 2007), and/or to the presence of artefacts (Bivolaru et al., 2022). Ceramic sherds and limestone fragments reworked from walls and pavements built along the stream banks could partly explain the very poor sorting of the sediments deposited in the channelized stream at LAP03 (Figs. 3, 10C).

A decrease in bedload accompanied with a progressive reduction of accommodation space and water depth began from the 2nd century CE, during which the flow dynamics could have been impacted by the accumulation of dump deposits then demolition materials (mainly tegulae) on the western bank (Figs. 9F, 10D). A mixture of suspended load and bedload with similar percentages of silt, fine sand and medium sand (ca. 25% each) was deposited in the channelized stream from the 2nd to the 4th centuries CE (Fig. 10D). A relatively higher macrocharcoal flux was recorded at LAP03 during this period, especially in the 3rd century CE (Fig. 11).

The sediments deposited in the abandoned stream (Sab) during the 5th and 6th centuries CE were characterized by a suspended load rich in silt and clay (ca. 45 and 25% on average, respectively) indicative of a low energy environment (Fig. 10E). Besides, the persistence of a shallow

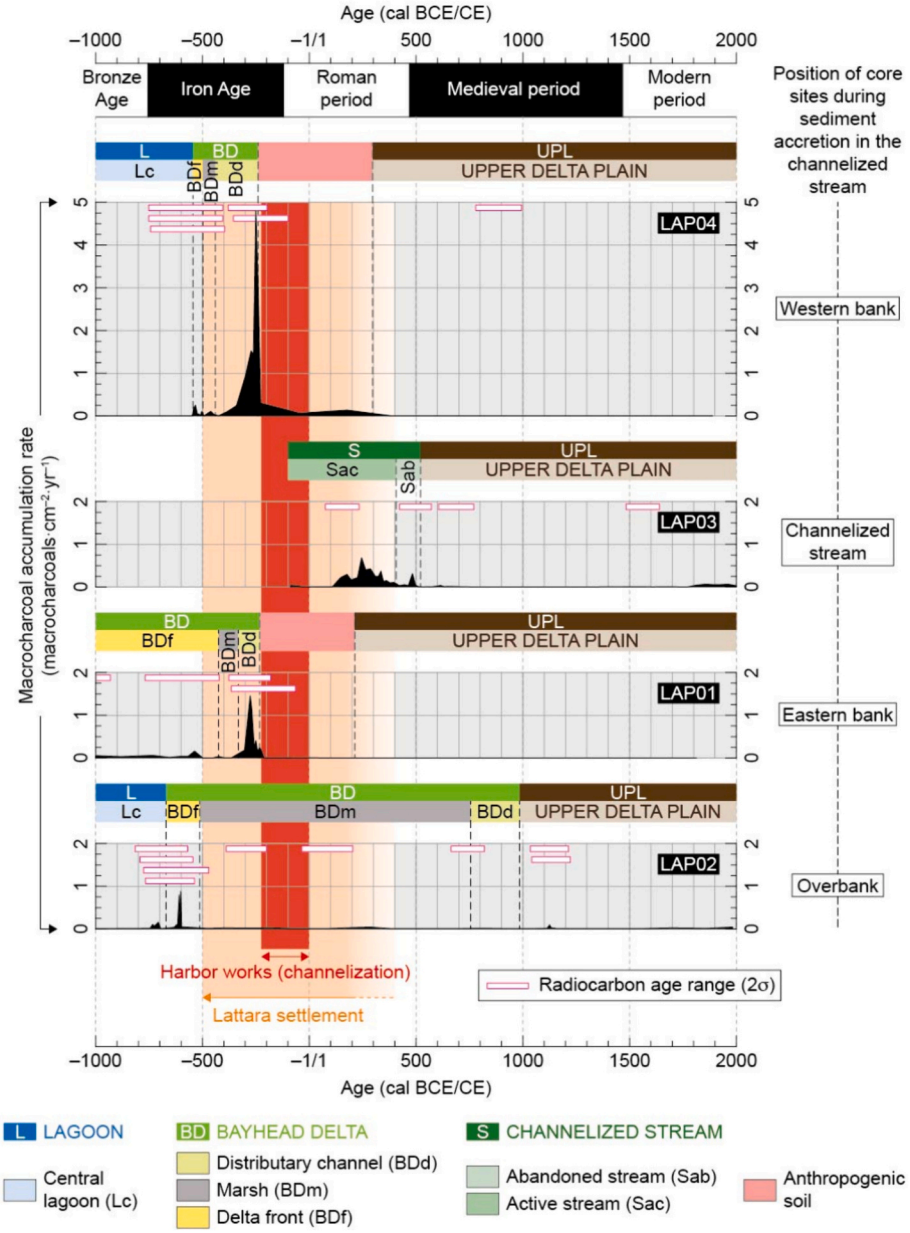

Fig. 11. Chronology of macrocharcoal accumulation rates in the sediments south of Lattara over the last 3000 years. Cultural periods from Blanchemanche et al. (2003).

brackish to freshwater marsh without significant terrigenous input until the early Middle Ages at LAP02 (Fig. 8), although the transition from the marsh BDm to distributary channel BDd occurred as soon as the 4th century BCE at LAP01 and LAP04 (Figs. 8, 9B), could be explained by the concentration of sediment flux in the channelized stream (Fig. 9.C–F), given that channelization may reduce lateral mobility of river sediments in ancient harbor areas (Salomon et al., 2017, 2018). This engineering solution might therefore have had a lasting impact on sedimentation and landscape evolution south of Lattara.

5.6. *Environmental factors*

The controlling factors of sediment dynamics and depositional energy in the deltaic area south of Lattara over the last 3000 years (Fig. 12A–B) may correspond to autogenic processes such as delta progradation or channel avulsion, anthropogenic forcing due to land use (e.g. channelization, urbanization, agriculture extension, Fig. 12C–E), and river flooding related to hydroclimatic conditions (Fig. 12F–I), which have changed along the coast of the Gulf of Lions over the last millennia (Blanchemanche, 2009; Degeai et al., 2017, 2022). More specifically, river floods due to extreme rainfall events were more frequent during periods of higher sea surface temperature (SST) and air temperature in the northwestern Mediterranean, as shown by instrumental data and documentary sources since the early 1900s (Degeai et al., 2022).

The relatively coarser grain size of sediments deposited between 1000 and 200 cal BCE was mainly driven by the progradation of the bayhead delta BD (Fig. 12A–B). The poor sorting of mouth bar sands (BDf, Fig. 10A) suggests an irregular flow possibly due to river flooding (Jorda, 2007; Bivolaru et al., 2022). The most proximal flood record available for the Late Bronze Age–Early Iron Age is in the Rhône delta (Fig. 1A), where flood-dominated regime occurred from 800 to 500 cal BCE (Arnaud-Fassetta et al., 2010). This is in agreement with a relatively high SST in the Gulf of Lions at this time (Fig. 12F), but not with negative anomalies of air temperature in northern Spain (Fig. 12G). Besides, the sediments deposited upstream of Lattara at Port Ariane and Céreirède (Fig. 1B) do not show evidence of increased flooding during this period (Blanchemanche et al., 2003; Jorda, 2007). Hence, further studies will be required to confirm the influence of river flooding and hydroclimatic changes on sedimentation south of Lattara in the first half of the last millennium CE (Fig. 12B).

Pollen data from Puertas (1998b) and Planchais et al. (1991) show the presence of vineyards east of the Lez delta plain near Pérols (Fig. 1B) and of cereal fields around Lattara after the foundation of this ancient city. Wine culture was particularly important in the second half of the last millennium BCE (Fig. 12E), and more specifically from the 3rd century BCE at Lattara and Port Ariane (Fig. 1B) (Daveau, 2007; Rovira and Alonso, 2018). Besides, grazing occurred around the harbor area of Lattara (Rovira et al., 2024). However, agriculture and pastoral activities do not seem to have had a significant impact on depositional energy and sediment size during this time interval (Fig. 12A–B).

Macrocharcoal accumulation rates were relatively high in the distributary channel deposits BDd dated from the 4th–3rd centuries BCE at LAP04 and LAP01, i.e. before the development of urbanization and channelization in the harbor area south of Lattara (Fig. 11). Macrocharcoal flux was particularly important at LAP04 where it was associated with anomalously high MS values (Fig. 6), which suggests that local fires occurred in the southern part of the city at this time. The chronology and spatial distribution of these anomalies could indicate that anthropogenic fires were triggered to prepare the harbor area for the construction of infrastructures, although further charcoal analyses will be required to study source areas, fire regimes and plant species.

Sediment dynamics from the 2nd century BCE to the 4th century CE was mainly driven by channelization that led to the concentration of bedload in the channelized stream between LAP04 and LAP01 (Fig. 12B). However, the coarsest particles deposited in this stream during the 1st century BCE and the 1st century CE (Fig. 12A, LAP03), as

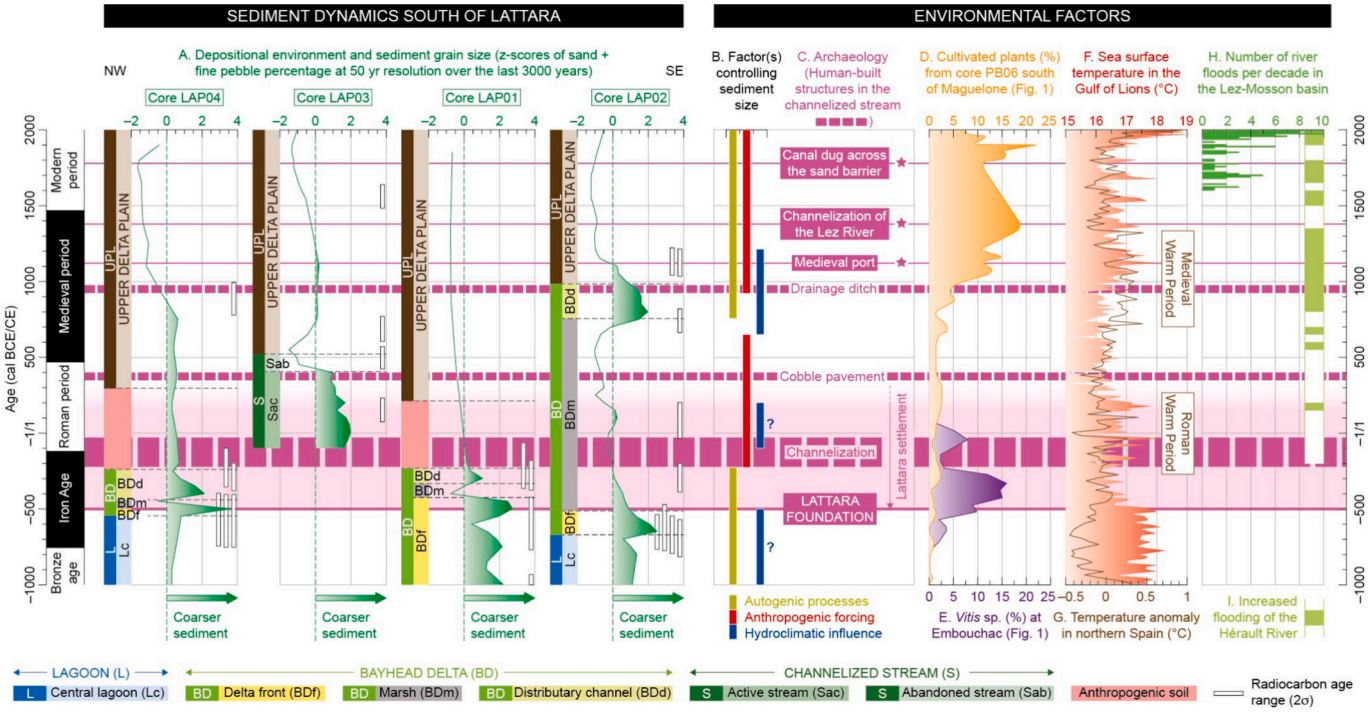

Fig. 12. Relationship between sediment dynamics, environmental changes and archaeological structures south of Lattara over the last 3000 years. Cultural periods from Blanchemanche et al. (2003). Data sources: A–B) this study; C) Blanchemanche (2000), Py (2009), Piquès (2016, 2019, 2022); D) Azuara et al. (2015); E) Puertas (1998a), with an age model obtained from a linear interpolation of radiocarbon dates of 2645 ± 55 BP at 330 cm depth (95.4% probability range of 928–591 cal BCE and median age of 818 cal BCE) and of 1740 ± 65 BP at 210 cm depth (95.4% probability range of 130–529 cal CE and median age of 319 cal CE); F) Jalali et al. (2018); G) Martin-Chivelet et al. (2011), sampled at 20-year resolution; H) Blanchemanche (2009) and Degeai et al. (2022) for the periods 1601–1800 and 1801–2000, respectively; I) Degeai et al. (2022).

well as the small increase in grain size underlined by a higher than average percentage of sand and fine pebble in the marsh at LAP02 during the 1st and 2nd centuries CE, coincided with increased flooding in the Hérault River basin west of Sète (Figs. 1A, 12I) and with flood-dominated regime in the Rhône delta (Arnaud-Fassetta, 2002). These phases of increased grain size and river flooding occurred in the Roman Warm Period that was characterized by relatively higher air and sea surface temperatures in the northwestern Mediterranean (Fig. 12F–G), whereas the deposition of finer-grained sediments in the channelized stream at LAP03 (Fig. 12A) and the decreased flooding in the Hérault basin (Fig. 12I) between the 3rd and 5th centuries CE were associated with lower temperatures (Fig. 12F–G).

Climate changes could therefore have influenced fluvial hydrology and depositional environment in Roman times (Fig. 12B), although the age of anthropogenic deposits in the channelized stream suggests that the decreasing particle size at LAP03 after the 2nd century CE was primarily driven by human activities (Fig. 12A–B). Indeed, the sharp decrease in the percentages of coarse sand and fine pebble (bedload) from the 2nd to the 4th centuries CE was synchronous with the accumulation of waste deposits and rubbles (tegulae and ceramic sherds) on the western bank (Figs. 9F, 10D), while the drastic increase in the percentages of silt and clay (suspended load) during the 5th and 6th centuries CE was preceded by the construction of cobble pavement SB205003 in the 4th century CE (Fig. 10D–E).

The deposition of coarser sediments was significantly strengthened at LAP03 and LAP02 from the 8th to the 11th centuries CE (Fig. 12A), which was approximately contemporaneous with the increase in particle size that occurred from the 6th to the 11th–12th centuries CE at Port Ariane upstream of Lattara (Fig. 1B), where it was deposited silty sand interbedded with coarse sand (Jorda, 2000, 2007). This could indicate increased fluvial activity and river flooding in the Lez delta plain during the Medieval Warm Period, perhaps under the influence of climate warming, as it was observed in the Hérault basin at the same time (Degeai et al., 2022) (Fig. 12G, I).

The late progradation of the bayhead delta and the formation of a distributary channel characterized by coarser sediments at LAP02 in the middle of the medieval period (Fig. 12A) indicate that the eastern branch of the Lez delta system (paleochannel 2b in Fig. 1B) was probably reactivated at this time. By contrast, the decreasing size of particles deposited between 800 and 1000 cal CE at LAP04 was probably due to the channel bifurcation of the Lez Viel stream toward the Robine des Marchands (channels 2a and 3 in Fig. 1B, respectively). Hence, autogenic processes coupled to hydroclimatic changes would have controlled the grain size of sediments south of Lattara during the first half of the medieval period (Fig. 12B).

Anthropogenic and geomorphic factors were the main drivers of sediment dynamics in the upper delta plain UPL during the second millennium CE (Fig. 12A–B). The westward avulsion of the Lez River led to the development of a distal floodplain dominated by the deposition of suspended clay and finer sediments in a low energy environment south of Lattara (Fig. 5, 12A). Documentary sources studied by Blanchemanche (2000, 2002) show that the river mouths of the Robine des Marchands and Lez Viel in the 11th–12th centuries CE were located about 500 m south and southwest of the ancient harbor of Lattara, respectively (Fig. 1B). Delta progradation was particularly rapid in the Lez delta plain over the last centuries. A southward shift of 2 km occurred between the 12th and 18th centuries CE for the river mouth of the Robine des Marchands after the abandonment of the Lez Viel channel, or between the late 14th and early 18th centuries CE for the mouth of the Lez River after its channelization in the second half of the 14th century CE, which resulted in relatively high progradation rates ranging between 3 and 6 m per year. The palaeogeographical changes necessarily related to this rapid progradation could have impacted human infrastructures in the Lez delta plain. For instance, the medieval port of Lattes was located about 500 m upstream of the river mouth of the Robine des Marchands at the time of its construction in the early 12th century CE, then at ca. 1 km less than one century later between 1250 and 1300 CE (Fig. 1B).

Besides, fluvial and runoff processes were impacted by land use at a local scale. For instance, the increasing flow discharge confined to the medieval ditch dug east of LAP03 during the 9th or 10th century CE (Figs. 9G, 12C), which was filled with relatively coarser sediments composed of sand and sandy silt (Piquès, 2017), could have impacted the energy of depositional environments in adjacent areas and explain the gradual decrease in the size of particles deposited at LAP02 (Fig. 12A). A ditch probably used to drain water also cut the sediments of the channelized stream in trench GAP6 from Arnal et al. (1974) (Fig. 2).

The digging of the medieval ditch occurred in a period of agricultural development characterized by increased expansion of cereal fields and cultivated trees (mainly chestnut, olive and walnut orchards) in the Lez coastal plain (Planchais and Parra Vergara, 1984; Azuara et al., 2015), as shown by the percentage of cultivated plants in core PB06 (Fig. 12D). Inhabited areas were widespread in humid environments such as coastal marshes from the late 10th century CE, and it was accompanied by an important impact on landscape with the development of land clearing, flow regulation, drainage works and water desalination (Durand, 2003). The construction of drainage and irrigation systems with a dense network of canals and ditches may allow intensive farming activities as well as the reduction of flood risk in urban areas (Marchetti, 2004). The reuse of the ancient channelized stream as a drainage ditch in a context of increased land use and river flooding during the Medieval Warm Period could therefore have contributed to reduce the effects of waterlogging in human settlements, cereal fields and tree orchards around Lattara.

6. Conclusion

The characterization of depositional environments and sedimentary processes around ancient cities in deltaic areas is important to understand the impact of coastal changes on archaeological structures and human activities, as well as past engineering solutions developed to maintain access to harbors in the face of delta progradation. The site of Lattara in southern France is a good example of ancient settlement influenced by deltaic progradation where engineering works were undertaken to reduce the effect of sediment accretion and waterlogging. A multi-proxy approach using sedimentological, palaeoecological and geochronological analyses of materials sampled in sediment cores and archaeological trenches was developed to study a channelized stream south of Lattara.

The lower delta plain was transgressed by a landward shift of the inner lagoon between 5000 and 4000 cal BCE, which led to the deposition of lagoonal sediments. The progradation of the Lez River delta system started around 1200 cal BCE in the study area and caused a sharp increase in sediment accumulation rates due to the formation of a bayhead delta. The upper part of this bayhead delta corresponds to a distributary channel formed in the 4th and 3rd centuries BCE south of Lattara. The water depth in this channel probably did not exceed a few decimeters at the end of the 3rd century BCE. Relative sea level during the channelization of the distributary channel at the transition between the 3rd and 2nd centuries BCE was estimated at -0.6 ± 0.2 m NGF. The water depth in the channelized stream would have reached ca. 3 m after channel deepening in the late 2nd century BCE.

Sedimentation was mainly controlled by autogenic processes due to delta progradation before the 2nd century BCE, then anthropogenic forcing caused by channelization led to an increase in sediment flux and bedload transport into the channelized stream. By contrast, harbor works and waste management in Late Antiquity could have led to a decrease in bedload transport. Besides, the strong expansion of cultivated areas that occurred around 1000 cal CE in a context of increased river flooding could explain the digging of a drainage ditch in the upper part of the sedimentary fill of the ancient channelized stream to adapt to environmental hazards.

Nevertheless, these potential human-environment interactions driven by land use or climate changes need to be confirmed by further geoarchaeological studies. More specifically, new geomorphological and geophysical investigations around Lattara and along the sandbar downstream of the Lez delta plain will be required to assess variations in flooded areas and water level changes during river floods or storm events in order to better characterize the impact of coastal flooding on archaeological structures.

Supplementary data to this article can be found online at https://doi.org/10.1016/j.margeo.2024.107384.

Credit authorship contribution statement

Jean-Philippe Degeai: Writing – original draft, Methodology, Formal analysis, Conceptualization. **Clémence Joseph:** Formal analysis. **Tiphaine Salel:** Formal analysis. **Matthieu Giaime:** Writing – original draft, Formal analysis. **Nuria Rovira:** Writing – original draft. **Gaël Piquès:** Writing – original draft, Conceptualization.

Declaration of competing interest

The authors declare that they have no known competing financial interests or personal relationships that could have appeared to influence the work reported in this paper.

Data availability

Data available at https://doi.org/10.17632/zy8fvvwfsb.1

Acknowledgments

This work was funded and supported by the LABEX ARCHIMEDE (Investissements d'Avenir ANR-11-LABX-0032-01, project PORTLAT: Environnements et ressources du port de *Lattara*), Région Occitanie (Défi Clé Sciences du Passé, project LittO), the French Ministry of Culture and Montpellier Méditerranée Métropole (project La zone portuaire de *Lattara*). Sedimentological and biological analyses were performed at the ArcheoEnvironnement technical platform of the Université Montpellier 3 and CNRS (UMR5140). The authors thank Paul Botte, Baptiste Lescalier and Tanguy Vallentin-Dulac for their contribution to sedimentological analyses, Séverine Sanz-Laliberte for the supply of topographic data, Ana Ejarque (ISEM UMR5554) for the supply of core S1, Benjamin P. Luley (Gettysburg College) for his contribution to radiocarbon dating, and Diane Dusseaux (Musée Henri Prades – Site archéologique *Lattara*) for the access to the archaeological site of Lattara. We also thank Pr. Edward Anthony (Editor) and two anonymous reviewers for their helpful comments and suggestions.

References

Ahmed, S., Bhattacharya, J.P., Garza, D.E., Li, Y., 2014. Facies architecture and stratigraphic evolution of a river-dominated delta front, Turonian Ferron Sandstone, Utah, U.S.A. J. Sediment. Res. 84, 97–121.

Ambert, P., 1999. Les formations littorales pléistocènes du Languedoc. Quaternaire 19, 21–28.

Ambert, M., Arthuis, R., 1995. L'évolution sédimentaire holocène de la basse vallée du Lez à l'aval de la cluse de Castelnau (Hérault). Archéologie en Languedoc 10 (2–3), 83–93.

Amorosi, A., Lucchi, M.R., Rossi, V., Sarti, G., 2009. Climate change signature of small-scale parasequences from Lateglacial–Holocene transgressive deposits of the Arno valley fill. Palaeogeogr. Palaeoclimatol. Palaeoecol. 273, 142–152.

Amorosi, A., Bini, M., Giacomelli, S., Pappalardo, M., Ribecai, C., Rossi, V., Sammartino, I., Sarti, G., 2013a. Middle to late Holocene environmental evolution of the Pisa coastal plain (Tuscany, Italy) and early human settlements. Quat. Int. 303, 93–106.

Amorosi, A., Rossi, V., Vella, C., 2013b. Stepwise post-glacial transgression in the Rhône Delta area as revealed by high-resolution core data. Palaeogeogr. Palaeoclimatol. Palaeoecol. 374, 314–326.

Amorosi, A., Bruno, L., Campo, B., Morelli, A., Rossi, V., Scarponi, D., Hong, W., Bohacs, K.M., Drexler, T.M., 2017. Global sea-level control on local parasequence architecture from the Holocene record of the Po Plain, Italy. Mar. Pet. Geol. 87, 99–111.

Anthony, E.J., Marriner, N., Morhange, C., 2014. Human influence and the changing geomorphology of Mediterranean deltas and coasts over the last 6000 years: from progradation to destruction phase? Earth Sci. Rev. 139, 336–361.

Arnal, J., Majurel, R., Prades, H., 1974. Le port de Lattara (Lattes, Hérault). Bordighera, Montpellier, p. 341.

Arnaud-Fassetta, G., 2002. Geomorphological records of a 'flood-dominated regime' in the Rhône Delta (France) between the 1st century BC and the 2nd century AD. What correlations with the catchment paleohydrology? Geodin. Acta 15, 79–92.

Arnaud-Fassetta, G., 2004. The upper Rhône Delta sedimentary record in the Arles–Piton core: analysis of delta-plain subenvironments, avulsion frequency, aggradation rate and origin of sediment yield. Geogr. Ann. A 86 (4), 367–383.

Arnaud-Fassetta, G., Carre, M.-B., Marocco, R., Maselli Scotti, F., Pugliese, N., Zaccaria, C., Bandelli, A., Bresson, V., Manzoni, G., Montenegro, M.E., Morhange, C., Pipan, M., Prizzon, A., Siché, I., 2003. The site of Aquileia (northeastern Italy): example of fluvial geoarchaeology in a Mediterranean deltaic plain. Geomorphologie 9 (4), 227–246.

Arnaud-Fassetta, G., Carcaud, N., Castanet, C., Salvador, P.-G., 2010. Fluviatile palaeoenvironments in archaeological context: Geographical position, methodological approach – Hydrological risk issues. Quat. Int. 216, 93–117.

Aschoff, J.L., Olariu, C., Steel, R.J., 2018. Recognition and significance of bayhead delta deposits in the rock record: a comparison of modern and ancient systems. Sedimentology 65, 62–95.

Athersuch, J., Horne, D., Whittaker, J., 1989. Marine and brackish water ostracods (superfami-lies Cypridacea and Cytheracea). In: Synopses of the British Fauna (New Series), 43, p. 343.

Azuara, J., Combourieu-Nebout, N., Lebreton, V., Mazier, F., Müller, S.D., Dezileau, L., 2015. Late Holocene vegetation changes in relation with climate fluctuations and human activity in Languedoc (southern France). Clim. Past 11, 1769–1784.

Bagan, G., Gailledrat, E., Jorda, C., 2010. Approche historique de la géographie des comptoirs littoraux à l'âge du Fer en Méditerranée occidentale à travers l'exemple du port de Lattara (Lattes, Hérault). Quaternaire 21 (1), 85–100.

Bertoncello, F., Devillers, B., Bonnet, S., Guillon, S., Bouby, L., Delhon, C., 2014. Mobilité des paysages littoraux et peuplement dans la basse vallée de l'Argens (Var, France) au cours de l'Holocène. Quaternaire 25 (1), 23–44.

Bhattacharya, J.P., 2024. Deltas. In: Posamentier, H.W., Walker, R.G. (Eds.), Facies Models Revisited, 84. SEPM Special Publication, pp. 237–292.

Bivolaru, A., Morhange, C., Stanica, A.D., Sava, T., Pascal, D., Mocanu, M., 2022. Geoarchaeological investigations of the river harbours of Noviodunum – the headquarters of the Roman Imperial fleet (Lower Danube, Romania). J. Archaeol. Sci. Rep. 45, 103614.

Blanchemanche, P., 2000. La plaine de Lattes du XII^{e} au XIX^{e} siècle. Dynamique naturelle et mise en valeur. Lattara 13, 198.

Blanchemanche, P., 2002. Les ports médiévaux de la plaine de Lattes. Quelques enseignements sur l'utilisation et l'aménagement des cours du Lez. Lattara 15, 203–211.

Blanchemanche, P., 2009. Crues historiques et vendanges en Languedoc méditerranéen oriental : la source, le signal et l'interprétation. Archéologie du Midi Médiéval 27, 225–235.

Blanchemanche, P., Berger, J.-F., Chabal, L., Jorda, C., Jung, C., Raynaud, C., 2003. Le littoral languedocien durant l'Holocène : milieu et peuplement entre Lez et Vidourle (Hérault, Gard). In: Muxart, T., Vivien, F.-D., Villalba, B., Burnouf, J. (Eds.), Des milieux et des hommes : fragments d'histoires croisées. Elsevier, Paris, pp. 79–92 collection environnement.

Blanchemanche, P., Chabal, L., Jorda, C., Jung, C., 2004. Le delta du Lez dans tous ses états : quels langages pour quel dialogue ? In: Burnouf, J., Leveau, P. (Eds.), Fleuves et marais, une histoire au croisement de la nature et de la culture. Comité des Travaux Historiques et Scientifiques, Paris, pp. 157–174.

Blott, S.J., Pye, K., 2001. GRADISTAT: a grain size distribution and statistics package for the analysis of unconsolidated sediments. Earth Surf. Process. Landf. 26, 1237–1248.

Boetto, G., 2010. Le port vu de la mer : l'apport de l'archéologie navale à l'étude des ports antiques. Bollettino di Archeologia online, Volume speciale 1 (B7), 112–128.

Boetto, G., 2016. Portus, Ostia and Rome: A transport zone in the maritime/land interface. In: Höghammar, K., Alroth, B., Lindhagen, A. (Eds.), Ancient Ports, the Geography of Connections, Proceedings of an International Conference at the Department of Archaeology and Ancient History, Uppsala University, 23–25 September 2010, vol. 34. Acta Universitatis Upsaliensis, Uppsala, Boreas, pp. 269–289.

Bonaduce, G., Ciampo, G., Masoli, M., 1975. Distribution of Ostracoda in the Adriatic Sea. Pubblicazioni della Stazione zoologica di Napoli 40, 154.

Bony, G., Morhange, C., Bruneton, H., Carbonel, P., Gébara, C., 2011. 2000 ans de colmatage du port antique de Fréjus (Forum Julii), France : une double métamorphose littorale. Compt. Rendus Geosci. 343, 701–715.

Brückner, H., Vött, A., Schriever, A., Handl, M., 2005. Holocene delta progradation in the eastern Mediterranean– case studies in their historical context. Méditerranée 104, 95–106.

Catuneanu, O., Galloway, W.E., Kendall, C.G., Miall, A.D., Posamentier, H.W., Strasser, A., Tucker, M.E., 2011. Sequence stratigraphy: methodology and nomenclature. Newsl. Stratigr. 44 (3), 173–245.

Chamberlain, E.L., Törnqvist, T.E., Shen, Z., Mauz, B., Wallinga, J., 2018. Anatomy of Mississippi Delta growth and its implications for coastal restoration. Sci. Adv. 4 (4), eaar4740.

Christol, M., 2010. Une histoire provinciale. La Gaule narbonnaise de la fin du II^{e} siècle av. J.-C. au III^{e} siècle ap. J.-C. Editions de la Sorbonne, Paris, p. 700.

Clanzig, S., 1987. Inventaire des invertébrés d'une lagune méditerranéenne des côtes de France, biocénoses et confinement : l'étang de Salses-Leucate (Roussillon). PhD thesis. EPHE, p. 466.
Clement, A.J.H., Fuller, I.C., 2018. Influence of system controls on the late Quaternary geomorphic evolution of a rapidly-infilled incised-valley system: the lower Manawatu valley, North Island New Zealand. Geomorphology 303, 13–29.
D'Angelo, G., Gargiullo, S., 1978. Guida alle conchiglie Mediterranee. Fabbri editori, Milan 223.
Daveau, I., 2007. Port Ariane (Lattes, Hérault). Contruction deltaïque et utilisation d'une zone humide lors des six derniers millénaires. Lattara 20, 640.
DDTM, 2013. Plan de prévention des risques naturels d'inondation. In: Commune de Lattes. Rapport de la Direction Départementale des Territoires et de la Mer de l'Hérault, Montpellier, p. 50.
De Graauw, A., 2022. Ancient Port Structures. Parallels between the Ancient and the Modern. Méditerranée. https://doi.org/10.4000/mediterranee.12715.
Dearing, J., 1999. Environmental magnetic susceptibility using the Bartington MS2 system. Bartington Instruments, Oxford, p. 43.
Degeai, J.-P., 2021. Les volcans agathois, témoins de l'évolution du relief littoral. Études Héraultaises 57, 73–88.
Degeai, J.-P., Devillers, B., Dezileau, L., Oueslati, H., Bony, G., 2015. Major storm periods and climate forcing in the Western Mediterranean during the Late Holocene. Quat. Sci. Rev. 129, 37–56.
Degeai, J.-P., Devillers, B., Blanchemanche, P., Dezileau, L., Oueslati, H., Tillier, M., Bohbot, H., 2017. Fluvial response to the last Holocene rapid climate change in the Northwestern Mediterranean coastlands. Glob. Planet. Chang. 152, 176–186.
Degeai, J.-P., Bertoncello, F., Vacchi, M., Augustin, L., De Moya, A., Ardito, L., Devillers, B., 2020. A new interpolation method to measure delta evolution and sediment flux: Application to the late Holocene coastal plain of the Argens River in the western Mediterranean. Mar. Geol. 424, 106159.
Degeai, J.-P., Blanchemanche, P., Tavenne, L., Tillier, M., Bohbot, H., Devillers, B., Dezileau, L., 2022. River flooding on the French Mediterranean coast and its relation to climate and land use change over the past two millennia. Catena 219, 106623.
Durand, A., 2003. Les paysages médievaux du Languedoc (X^{e}-XII^{e} siècles). Presses Universitaires du Midi, Toulouse, p. 480.
Edmonds, D.A., Slingerland, R.L., 2007. Mechanics of river mouth bar formation: implications for the morphodynamics of delta distributary networks. J. Geophys. Res. 112, F02034.
Fagherazzi, S., Edmonds, D.A., Nardin, W., Leonardi, N., Canestrelli, A., Falcini, F., Jerolmack, D.J., Mariotti, G., Rowland, J.C., Slingerland, R.L., 2015. Dynamics of river mouth deposits. Rev. Geophys. 53, 642–672.
Faïsse, C., Mathé, V., Bruniaux, G., Labussière, J., Cavero, J., Jézégou, M.-P., Lefèvre, D., Sanchez, C., 2018. Palaeoenvironmental and archaeological records for the reconstruction of the ancient landscape of the Roman harbour of Narbonne (Aude, France). Quat. Int. 463, 124–139.
Flaux, C., Carayon, N., Faïsse, C., Guy, M., Salel, T., Sanchez, C., 2020. Géoarchéologie de Port-la-Nautique (étangs narbonnais). Méditerranée. https://doi.org/10.4000/mediterranee.11732.
Folk, R.L., Ward, W.C., 1957. Brazos River bar: a study in the significance of grain size parameters. J. Sediment. Petrol. 27 (1), 3–26.
Fuhrmann, R., 2013. Atlas quartärer und rezenter Ostrakoden Mitteldeutschlands, 15. Altenburger Naturwissenschaftliche Forschungen, p. 320.
Garcia, D., 2008. Le port de Lattara (Lattes, Hérault) : premiers acquis sur les phases préromaines et romaines. Gallia 65, 131–149.
Garcia, D., Vallet, L., 2002. L'espace portuaire de Lattes antique. Lattara 15, 223.
Garmony, O., Ripken, T.E.J., 2011. Une collection de reference pour la malacofauna terrestre de France. MalaCo, Hors Série, 1, pp. 1–108.
Gébara, C., Morhange, C., 2010. Fréjus (Forum Julii): le port antique/the ancient harbour. J. Roman Archaeol. Suppl. 77, 152.
Giaime, M., Morhange, C., Cau Ontiveros, M.A., Fornos, J.J., Vacchi, M., Marriner, N., 2017. In search of Pollentia's southern harbour: Geoarchaeological evidence from the Bay of Alcúdia (Mallorca, Spain). Palaeogeogr. Palaeoclimatol. Palaeoecol. 466, 184–201.
Giaime, M., Marriner, N., Morhange, C., 2019. Evolution of ancient harbours in deltaic contexts: a geoarchaeological typology. Earth Sci. Rev. 191, 141–167.
Giraudi, C., Tata, C., Paroli, L., 2009. Late Holocene Evolution of Tiber River Delta and Geoarchaeology of Claudius and Trajan Harbor, Rome. Geoarchaeology 24 (3), 371–382.
Glöer, P., Meier-Brook, C., 1998. Süsswassermollusken. Ein Bestimmungsschlüssel für die Bundesrepublik Deutschland. Deutscher Jugendbund für Naturbeobachtung, Hamburg, p. 136.
Goiran, J.-P., Tronchère, H., Salomon, F., Carbonel, P., Djerbi, H., Ognard, C., 2010. Palaeoenvironmental reconstruction of the ancient harbors of Rome: Claudius and Trajan's marine harbors on the Tiber delta. Quat. Int. 216, 3–13.
Jalali, B., Sicre, M.-A., Klein, V., Schmidt, S., Maselli, V., Lirer, F., Bassetti, M.-A., Toucanne, S., Jorry, S.J., Insinga, D.D., Petrosino, P., Châles, F., 2018. Deltaic and coastal sediments as recorders of Mediterranean regional climate and human impact over the past three millennia. Paleoceanography 33, 579–593.
Jorda, C., 2000. Morphogenèse alluviale et aménagements dans la plaine deltaïque du Lez depuis 6000 ans : la fouille archéologique de sauvetage de Port-Ariane (Lattes, Hérault). Méditerranée 94 (1–2), 25–32.
Jorda, C., 2002. La zone portuaire de Lattara, entre Lez et étang. Indices d'un rivage lagunaire aux alentours du changement d'ère. Lattara 15, 171–180.
Jorda, C., 2007. Morphogenèse alluviale et paléogéographie d'un paysage deltaïque : le cas de Port Ariane. Lattara 20, 47–87.
Jorda, C., Chabal, L., Blanchemanche, P., 2008. Lattara entre terres et eaux : paléogéographie et paléoboisements autour du port protohistorique. Gallia 65, 11–21.
Kerney, M.P., Cameron, R.A.D., 2006. Guide des escargots et limaces d'Europe. Delachaux et Niestlé Eds, Paris, p. 370.
La Rivière, M., Michez, N., Delavenne, J., Andres, S., Fréjefond, C., Janson, A.-L., Abadie, A., Amouroux, J.-M., Bellan, G., Bellan-Santini, D., Chevaldonné, P., Cimiterra, N., Derolez, V., Fernez, T., Fourt, M., Frisoni, F., Grillas, P., Harmelin, J.-G., Jordana, E., Klesczewski, M., Labrune, C., Mouronval, J.-B., Ouisse, V., Palomba, L., Pasqualini, V., Pelaprat, C., Pérez, T., Pergent, G., Pergent-Martini, C., Sartoretto, S., Thibaut, T., Vacelet, J., Verlaque, M., 2021. Fiches descriptives des biocénoses benthiques de Méditerranée. UMS PatriNat (OFB-CNRS-MNHN), Paris, p. 660.
Lisé-Pronovost, A., Salomon, F., Goiran, J.-P., St-Onge, G., Herries, A.I.R., Montero-Serrano, J.-C., Heslop, D., Roberts, A.P., Levchenko, V., Zawadzki, A., Heijnis, H., 2019. Dredging and canal gate technologies in Portus, the ancient harbour of T Rome, reconstructed from event stratigraphy and multi-proxy sediment analysis. Quat. Int. 511, 78–93.
Marchetti, M., 2004. Flow regulation systems. In: Goudie, S.A. (Ed.), Encyclopedia of Geomorphology. Taylor & Francis, New York, pp. 384–387.
Marlier, S., 2018. Navires et navigations dans le delta du Rhône à l'époque romaine. Archaeonautica 20, 103–140.
Marriner, N., Morhange, C., 2007. Geoscience of ancient Mediterranean harbours. Earth Sci. Rev. 80, 137–194.
Martin-Chivelet, J., Munoz-Garcia, M.B., Edwards, R.L., Turrero, M.J., Ortega, A.I., 2011. Land surface temperature changes in Northern Iberia since 4000 yr BP, based on δ^{13}C of speleothems. Glob. Planet. Chang. 77, 1–12.
Meisch, C., 2000. Freshwater Ostracoda of Western and Central Europe. Spektrum Akademischer Verlag, Heidelberg, p. 521.
Millspaugh, S.H., Whitlock, C., 1995. A 750-year fire history based on lake sediment records in central Yellowstone National Park, USA. Holocene 5 (3), 283–292.
Morhange, C., Marriner, N., Baralis, A., Blot, M.L., Bony, G., Carayon, N., Carmona, P., Flaux, C., Giaime, M., Goiran, J.-P., Kouka, M., Lena, A., Oueslati, A., Pasquinucci, M., Porotov, A., 2015. Dynamiques géomorphologiques et typologie géoarchéologique des ports antiques en contextes lagunaires. Quaternaire 26 (2), 117–139.
Oertli, H.J., 1985. Atlas de ostracodes de France. Mémoires Elf-Aquitaine 9, 396.
Passega, R., 1964. Grain size representation by CM patterns as a geological tool. J. Sediment. Petrol. 34 (4), 830–847.
Passega, R., Byramjee, R., 1969. Grain-size image of clastic deposits. Sedimentology 13, 233–252.
Patterson, W.A., Edwards, K.J., Maguire, D.J., 1987. Microscopic charcoal as a fossil indicator of fire. Quat. Sci. Rev. 6, 3–23.
Piquès, G., 2016. Lattara (Lattes, Hérault). Prospections géophysiques et sondages géoarchéologiques dans la zone portuaire. In: Archaeological Report, Occitanie Pyrénées-Méditerranée, p. 135.
Piquès, G., 2017. La zone portuaire de Lattara (Lattes, Hérault). Archaeological report, DRAC Occitanie Pyrénées-Méditerranée, p. 192.
Piquès, G., 2019. La zone portuaire de Lattara (Lattes, Hérault). Archaeological report, DRAC Occitanie Pyrénées-Méditerranée, p. 497.
Piquès, G., 2020. La zone portuaire de Lattara (Lattes, Hérault). Archaeological report, DRAC Languedoc-Roussillon, p. 264.
Piquès, G., 2022. La zone portuaire de Lattara (Lattes, Hérault). Archaeological report, DRAC Occitanie, p. 246.
Planchais, N., Parra Vergara, I., 1984. Analyses polliniques de sédiments lagunaires et côtiers en Languedoc, en Roussillon et dans la province de Castellon (Espagne). Bioclimatologie. B. Soc. Bot. Fr.-Actual. 131 (2–4), 97–105.
Planchais, N., Duzer, D., Fontugne, M., 1991. Palynologie de dépôts holocènes de Lattes (Hérault). C.R. Acad. Sci. II 313, 1357–1360.
Ponce, J.J., Carmona, N., Jait, D., Cevallos, M., Rojas, C., 2024. Sedimentological and ichnological characterization of delta front mouth bars in a river-dominated delta (Upper cretaceous) from the La Anita Formation, Austral Basin, Argentina. Sedimentology 71, 27–53.
Puertas, O., 1998a. Évolution holocène de la végétation en bordure de l'étang de Méjean : analyse pollinique du sondage d'Embouchac (Lattes, Hérault, France). Quaternaire 9 (2), 79–89.
Puertas, O., 1998b. Palynologie dans le delta du Lez. Contribution à l'histoire du paysage de Lattes. Lattara 11, 181.
Py, M., 1988. Sondages dans l'habitat antique de Lattes. Les fouilles d'Henri Prades et du Groupe Archéologique Painlevé (1963-1985). Lattara 1, 65–146.
Py, M., 2009. Lattara. Lattes, Hérrault. Comptoir gaulois méditerranéen entre Etrusques, Grecs et Romains. Editions errance, Paris, p. 343.
Py, M., Garcia, D., 1993. Bilan des recherches archéologiques sur la ville portuaire de Lattara (Lattes, Hérault). Gallia 50, 1–93.
Py, M., Adroher Auroux, A.M., Sanchez, C., 2001. Corpus des céramiques de l'âge du Fer de Lattes (fouilles 1963-1999). Lattara 14 (1), 1–612.
Raynal, O., Bouchette, F., Certain, R., Séranne, M., Dezileau, L., Sabatier, P., Lofi, J., Bui Xuan Hy, A., Briqueu, L., Pezard, P., Tessier, B., 2009. Control of alongshore-oriented sand spits on the dynamics of a wave-dominated coastal system (Holocene deposits, northern Gulf of Lions, France). Mar. Geol. 264, 242–257.
Raynal, O., Bouchette, F., Certain, R., Sabatier, P., Lofi, J., Seranne, M., Dezileau, L., Briqueu, L., Ferrer, P., Courp, T., 2010. Holocene evolution of a Languedocian lagoonal environment controlled by inherited coastal morphology (northern Gulf of Lions, France). B. Soc. Geol. Fr. 181 (2), 211–224.
Reimer, P.J., Austin, W.E.N., Bard, E., Bayliss, A., Blackwell, P.G., Bronk Ramsey, C., Butzin, M., Cheng, H., Edwards, R.L., Friedrich, M., Grootes, P.M., Guilderson, T.P.,

Hajdas, I., Heaton, T.J., Hogg, A.G., Hughen, K.A., Kromer, B., Manning, S.W., Muscheler, R., Palmer, J.G., Pearson, C., van der Plicht, J., Reimer, R.W., Richards, D.A., Scott, E.M., Southon, J.R., Turney, C.S.M., Wacker, L., Adolphi, F., Büntgen, U., Capano, M., Fahrni, S.M., Fogtmann-Schulz, A., Friedrich, R., Köhler, P., Kudsk, S., Miyake, F., Olsen, J., Reinig, F., Sakamoto, M., Sookdeo, A., Talamo, S., 2020. The IntCal20 northern hemisphere radiocarbon age calibration curve (0–55 cal kBP). Radiocarbon 62, 725–757.

Rousse, C., Fontaine, S., Landuré, C., Marty, F., Quesnel, Y., Vella, C., Dussouillez, P., Fleury, J., Uehara, M., 2020. Le canal de Marius : réflexions autour d'une nouvelle hypothèse de tracé dans le secteur des Marais du Vigueirat. Rev. Archeol. Narbonnaise 52, 109–120.

Rovira, N., Alonso, N., 2018. Crop growing and plant consumption in coastal Languedoc (France) in the Second Iron Age: new data from Pech Maho (Aude), Lattara (Hérault) and Le Cailar (Gard). Veg. Hist. Archaeobotany 27 (1), 85–97.

Rovira, N., Steiner, B.L., Tillier, M., Degeai, J.-P., Joseph, C., Ejarque, A., Liottier, L., Jorda, C., Martin, S., Riera, S., Piquès, G., 2024. Environnements et activités humaines à Lattara (Hérault, France) entre la fin de l'âge du Fer et le Haut-Empire romain (fin IIIe s. av. n. è.-IIe s. de n. è.) : premiers résultats archéologiques, géomorphologiques, archéobotaniques et malacologiques issus du canal de la zone portuaire (campagnes 2016-2020). In: Chevalier, A., Court-Picon, M., Preiss, S., Speleers, L. (Eds.), Actualités, Méthodologies, Terroirs, Synergies, Actes des 14e Rencontres d'Archéobotanique en Langue Française, Bruxelles, 13-16 Octobre 2021. Presses Universitaires de Louvain.

Salel, T., Bruneton, H., Lefèvre, D., 2016. Ostracods and environmental variability in lagoons and deltas along the North-Western Mediterranean coast (Gulf of Lions, France and Ebro delta, Spain). Rev. Micropaleontol. 59, 425–444.

Salel, T., Bruneton, H., Degeai, J.-P., Mulot, M., Lefèvre, D., 2019. Nouvelles données sur la dynamique des environnements fluvio-lagunaires de la basse vallée de l'Aude (France) au cours des sept derniers millénaires. Quaternaire 30 (4), 351–368.

Salel, T., Flaux, C., Bruneton, H., Degeai, J.-P., Devillers, B., Lefèvre, D., 2020. Changements du niveau marin relatif à l'Holocène ancien et moyen sur la côte du Golfe du Lion. Quaternaire 31 (1), 33–44.

Salomon, F., Purdue, L., Goiran, J.-P., Berger, J.-F., 2014a. Introduction to the special issue: Roman canals studies—main research aims. Water Hist. 6, 1–9.

Salomon, F., Goiran, J.-P., Bravard, J.-P., Arnaud, P., Djerbi, H., Kay, S., Keay, S., 2014b. A harbour–canal at Portus: a geoarchaeological approach to the Canale Romano: Tiber delta, Italy. Water Hist. 6, 31–49.

Salomon, F., Keay, S., Carayon, N., Goiran, J.-P., 2016. The Development and Characteristics of Ancient Harbours—applying the PADM Chart to the Case Studies of Ostia and Portus. PLoS One 11 (9), e0162587.

Salomon, F., Goiran, J.-P., Pannuzi, S., Djerbi, H., Rosa, C., 2017. Long-Term Interactions between the Roman City of Ostia and its Paleomeander, Tiber Delta, Italy. Geoarchaeology 32, 215–229.

Salomon, F., Goiran, J.-P., Noirot, B., Pleuger, E., Bukowiecki, E., Mazzini, I., Carbonel, P., Gadhoum, A., Arnaud, P., Keay, S., Zampini, S., Kay, S., Raddi, M., Ghelli, A., Pellegrino, A., Morelli, C., Germoni, P., 2018. Geoarchaeology of the Roman port-city of Ostia: Fluvio-coastal mobility, urban development and resilience. Earth Sci. Rev. 177, 265–283.

Salomon, F., Strutt, K., Mladenovic, D., Goiran, J.-P., Keay, S., 2023. Management of fluvio-coastal dynamics in the Tiber delta during the Roman period: using an integrated waterways system to cope with environmental challenges at Ostia and Portus. Water Hist. 15, 105–123.

Sanchez, C., Labussière, J., Jézégou, M.P., Mathé, V., Mathieu, V., Cavero, J., 2016. L'embouchure du fleuve antique dans les étangs narbonnais. In: Sanchez, C., Jézégou, M.-P. (Eds.), Les ports dans l'espace méditerranéen antique. Narbonne et les systèmes portuaires fluvio-lagunaires. Rev. Archeol. Narbonnaise, Suppl. 44, Montpellier, pp. 59–69.

Schumm, S.A., 1963. A Tentative Classification of Alluvial River Channels. US Department of the Interior, Washington, Geological Survey Circular, 477, p. 10.

Stock, F., Knipping, M., Pint, A., Ladstätter, S., Delile, H., Heiss, A.G., Laermanns, H., Mitchell, P.D., Ployer, R., Steskal, M., Thanheiser, U., Urz, R., Wennrich, V., Brückner, H., 2016. Human impact on Holocene sediment dynamics in the Eastern Mediterranean – the example of the Roman harbour of Ephesus. Earth Surf. Process. Landf. 41 (7), 980–996.

Stock, F., Halder, S., Opitz, S., Pint, A., Seren, S., Ladstätter, S., Brückner, H., 2019. Late Holocene coastline and landscape changes to the west of Ephesus, Turkey. Quat. Int. 501, 349–363.

Stuiver, M., Reimer, P.J., 1993. Extended ^{14}C data base and revised CALIB 3.0 ^{14}C age calibration program. Radiocarbon 35 (1), 215–230.

Vacchi, M., Marriner, N., Morhange, C., Spada, G., Fontana, A., Rovere, A., 2016. Multiproxy assessment of Holocene relative sea-level changes in the western Mediterranean: Sea-level variability and improvements in the definition of the isostatic signal. Earth Sci. Rev. 155, 172–197.

Vachula, R.S., Russell, J.M., Huang, Y., Richter, N., 2018. Assessing the spatial fidelity of sedimentary charcoal size fractions as fire T history proxies with a high-resolution sediment record and historical data. Palaeogeogr. Palaeoclimatol. Palaeoecol. 508, 166–175.

Van der Plicht, J., 2004. Radiocarbon, the calibration curve and Scythian chronology. In: Scott, E.M., Alekseev, A.Y., Zaitseva, G. (Eds.), Impact of the Environment on Human Migration in Eurasia. NATO Science Series, IV Earth and Environmental Sciences 42. Springer, Netherlands, pp. 45–61.

Vella, C., Leveau, P., Provansal, M., Gassend, J.-M., Maillet, B., Sciallano, M., 1999. Le canal de Marius et les dynamiques littorales du golfe de Fos. Gallia 56, 131–139.

Vött, A., Willershäuser, T., Hadler, H., Obrocki, L., Fischer, P., Heinzelmann, M., 2020. Geoarchaeological evidence of Ostia's river harbour operating until the fourth century AD. Archaeol. Anthropol. Sci. 12, 88.

Welter-Schultes, F., 2012. European non-marine molluscs, a guide for species identification. Planet Poster Editions, Göttingen, p. 760.

Whitlock, C., Larsen, C.P.S., 2001. Charcoal as a fire proxy. In: Smol, J.P., Birks, H.J.B., Last, W.M. (Eds.), Tracking Environmental Change Using Lake Sediments. Volume 3: Terrestrial, Algal, and Siliceous Indicators. Kluwer Academic Publishers, Dordrecht, pp. 75–97.

Zhang, K., Wu, S.-H., Wang, J.-J., Xu, Y.-J., Xu, Z.-H., Zhang, J.-J., 2022. Vertical grain-size trend of mouth bar in lacustrine fan delta: Flume experiments. Pet. Sci. 19, 1964–1977.

Zielhofer, C., Bussmann, J., Ibouhouten, H., Fenech, K., 2010. Flood frequencies reveal Holocene rapid climate changes (Lower Moulouya River, northeastern Morocco). J. Quat. Sci. 25 (5), 700–714.